HIGH RESOLUTION STUDY OF THE ÅNGSTRÖM BAND SYSTEM OF THE $^{13}C^{18}O$ MOLECULE

CHINTALAPATI V. V. PRASAD

HIGH RESOLUTION STUDY OF THE ÅNGSTRÖM BAND SYSTEM OF THE $^{13}C^{18}O$ MOLECULE

BY

Chintalapati V. V. Prasad

A thesis submitted to the School of Graduate Studies in partial fulfillment of the requirements for the degree of Master of Science

Department of Physics

Memorial University of Newfoundland

April 1983

St.John's Newfoundland

ACKNOWLEDGMENTS

I wish to express my sincere gratitude to my supervisor, Prof. S.P.Reddy, for his constant encouragement and guidance through all stages of this thesis.

I am grateful to Dr. G.L.Bhale for his excellent help during the experimental stage and also for the useful discussions. I would like to thank Dr. P.P. Narayanaswami, Department of Mathematics, Mr. P. Gillard, and Mr. E. van Nostrand for helpful discussions in computer programming. My thanks are also due to the following technical personnel for their invaluable assistance : Messers T.G. White and M. Ryan for the mechanical work, D. Seymour, M. Hatswell, and T. Perks for their skillful glassblowing, A.W. McCloy for his help in the construction of the power supplies, R. Guest for drafting some diagrams, R. Bradley for some photographic work, and Mrs. B. Burke for some typing.

The financial support received from the Memorial University of Newfoundland in the form of Graduate Fellowship and Graduate Teaching Assistantship, and bursary from Dr. S.P. Reddy's NSERC grant are gratefully acknowledged.

ABSTRACT

A hollow cathode discharge tube of special design whose cathode portion can be conveniently cooled with liquid nitrogen during the operation of the discharge was constructed. Initial experiments have shown that the cathode glow is an excellent source to obtain the electronic band spectra of several **ionic** diatomic molecules and that the anode glow is a convenient source to obtain certain selective diatomic band systems of numerous **neutral** diatomic molecules.

The $B\,^1\Sigma^+ - A\,^1\Pi$ Ångström band system of the $^{13}C\,^{18}O$ molecule consisting of eight bands in the region 4100 - 6500 Å was photographed under the medium dispersion of a 2 m Bausch and Lomb dual grating spectrograph in the first order of a 600 grooves/mm grating as well as under the high resolutions of this instrument and a 3.4 m Jarrell - Ash Ebert grating spectrograph, in each case, in the second and third orders of a 1200 grooves/mm grating.

Detailed rotational analysis has been carried out for the first time for the 1-0, 1-1, 0-1, 0-2, 0-3, 0-4, and 0-5 bands except for the complex 0-0 band. Rotational constants for both $A\,^1\Pi$ and $B\,^1\Sigma^+$ states as well as the origins of these bands have been derived from the analysis. Vibrational constants for the two states are also obtained from the band origins.

Perturbations observed in the vibrational levels v = 0, 3, and 5 of the

$A\,^1\Pi$ state have been analyzed in detail. It is found that the v = 0 level of the A state is perturbed by the v = 1 level of the $e\,^3\Sigma^-$ state and its v = 3 and 5 levels are perturbed by the v = 13 and 16 levels of the $a'\,^3\Sigma^+$, respectively.

CONTENTS

CHAPTER 1

INTRODUCTION

The experimental investigations of the electronic band spectra of diatomic molecules and their theoretical interpretations have been greatly accelerated with the development of the quantum theory in the late 1920's. From a detailed analysis of the electronic spectrum of a molecule, its electronic, vibrational, and rotational levels can be derived very precisely. Also from these, one can obtain a detailed information about the electronic structure of the molecule and the vibration and rotation of its nuclei. An insight into the important properties like chemical valence can be achieved from the electronic configuration. The forces between the atoms of a molecule and its dissociation energy can be calculated from the vibrational frequencies and the corresponding anharmonicities. From a study of the rotational structure of the electronic band spectra of a diatomic molecule, information about the internuclear distance and the nature of the coupling between the electronic and rotational motions of the molecules can be obtained. The information concerning the perturbations occurring between the energy levels of various electronic states can also be obtained from a study of the rotational structure of the bands. Thus the study of the electronic spectra of a molecule enables us to understand its various physical and chemical properties.

1.1 Electronic States of Carbon Monoxide

The electrons in the outermost shells of the constituent atoms of a molecule determine the type of moleculer binding and the nature of the molecular states. The ground state electronic configurations of the carbon and oxygen atoms which form the carbon monoxide molecule are:

$$C: K\ 2s^2\ 2p^2\ ;\quad O: K\ 2s^2\ 2p^4$$

The electronic configuration which gives rise to the ground state $X^1\Sigma^+$ of the CO molecule is written as (Mulliken, 1932)

$$K\ K\ (z\sigma)^2\ (y\sigma)^2\ (w\pi)^4\ (x\sigma)^2\ :\ X^1\Sigma^+ \qquad (1.1)$$

The electronic configurations of the low-lying excited states of CO can be written by promoting (i) one of the $x\sigma$ electrons to the $v\pi$ orbital and (ii) one of the $w\pi$ electrons to the $v\pi$ orbital. Following the notation of the Hund (1930) and Mulliken (1932), the resulting electronic configurations and states are written as

$$-\ -\ -\ -\ (w\pi)^4\ (x\sigma)\ (v\pi)\ :\ {}^3\Pi_r,\ {}^1\Pi \qquad (1.2)$$

$$-\ -\ -\ -\ (w\pi)^3\ (x\sigma)^2\ (v\pi)\ :\ {}^3\Sigma^+,\ {}^3\Sigma^-,\ {}^3\Delta_i,\ {}^1\Sigma^+,\ {}^1\Sigma^-,\ {}^1\Delta. \qquad (1.3)$$

For the CO molecule the electronic states of the Configurations (1.2) and (1.3) have been identified as the $a^3\Pi_r$ and $A\,^1\Pi$ and $a',^3\Sigma^+$, $e^3\Sigma^-$, $d^3\Delta_i$, $I^1\Sigma^-$, and $D^1\Delta$ states respectively. But the $^1\Sigma^+$ state of Configuration (1.3) has not yet been observed. Further excited state electronic configurations of CO are obtained by raising once one of the x σ electrons of Configuration (1.1) to the $u\sigma$ orbital and later one of the $w\pi$ electrons to the $u\sigma$ orbital as given below :

$$- - - - (w\pi)^4 \ (x\sigma) \ (u\sigma) \ : \ {}^3\Sigma^+, \ {}^1\Sigma^+ \qquad (1.4)$$

$$- - - - (w\pi)^3 \ (x\sigma)^2 \ (u\sigma) \ : \ {}^3\Pi_i, \ {}^1\Pi \qquad (1.5)$$

None of these four states have been observed so far. Further excited states of CO are obtained by promoting one of the $x\sigma$ electrons to the Rydberg orbitals $3s\sigma$, $3p\sigma$, and $3p\pi$, etc. The resulting states are identified as :

$$- - - - (w\pi)^4 \ (x\sigma) \begin{cases} 3s\sigma : b\,{}^3\Sigma^+, \ B\,{}^1\Sigma^+ \\ 3p\sigma : j\,{}^3\Sigma^+, \ C\,{}^1\Sigma^+ \\ 3p\pi : c\,{}^3\Pi_i, \ E\,{}^1\Pi \end{cases}$$

Finally these Rydberg states converge to the ground state ($X^2\Sigma^+$) of the CO^+ molecule (Lefebvre - Brion *et al* 1964). For more details of all the electronic states and other spectroscopic details of the CO molecule, the reader is referred to Krupenie (1966), Tilford and Simmons (1972), and Huber and Herzberg (1979) and the references therein. The Rydberg - Klein - Rees (RKR) potential energy curves of all observed states of $^{12}C\,^{16}O$ below 11.77 ev are reproduced in Fig.1 from Tilford and Simmons (1972). From this figure it is noticed that the states X, a, a', d, e, A, I, and D dissociate into $C(^3P)$ and $O(^3P)$ atoms.

Molecular physicists and chemists consider carbon monoxide to be one of the important molecules for the following reasons: (i) its spectrum can be readily excited by different excitation mechanisms; (ii) it is one of the products of combustion of organic molecules; (iii) the solar chromosphere, stellar atmospheres and comets contain carbon monoxide in appreciable quantities; (iv) it is isoelectronic with molecular nitrogen which is the principal

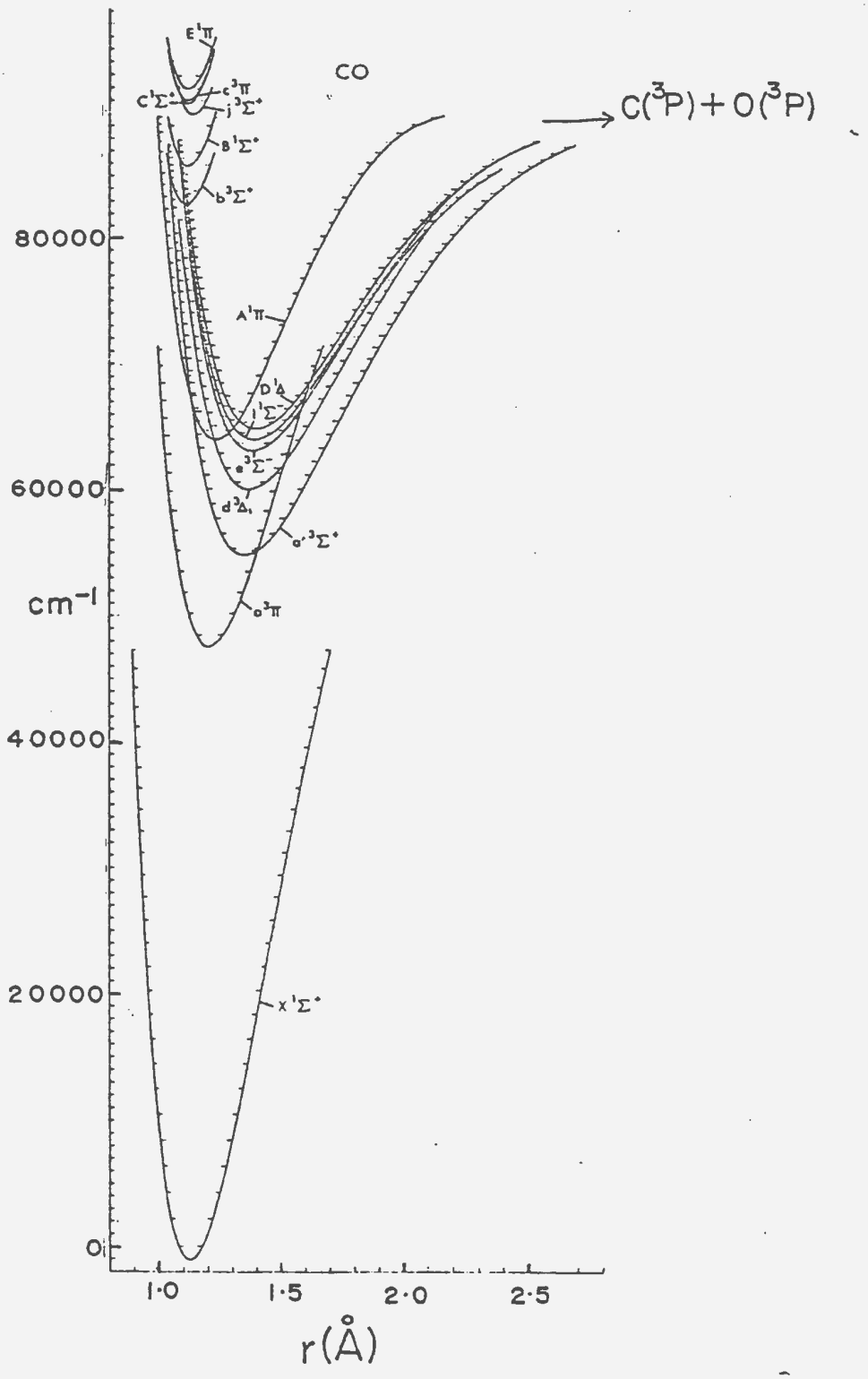

Fig. 1. Potential energy curves for the electronic states of $^{12}C\,^{16}O$ below 11.77 ev.

constituent of the earth's atmosphere; (v) it is amenable to theoretical numerical calculations of properties such as energy of electronic states, ionization potentials, and nature of the electronic states etc., and (vi) it can be readily handled in the laboratory.

Extensive experimental studies have been made both in emission and absorption on the electronic spectrum of the $^{12}C^{16}O$ molecule which spans the region 600 - 8600 Å. In total 30 electronic transitions are found among the 24 known states of $^{12}C^{16}O$. Of these 30, the three prominent band systems are (i) the $B\,^1\Sigma^+ - A\,^1\Pi$ Ångström system (4100 - 6600 Å), (ii) the $b\,^3\Sigma^+ - a\,^3\Pi$ Third Positive system (2600 - 3800 Å), and (iii) the $A\,^1\Pi - X\,^1\Sigma^+$ Fourth Positive system (1140 - 2800 Å). The Ångström system and the Fourth Positive system have also been observed in the isotopically substituted molecules $^{13}C^{16}O$ and $^{12}C^{18}O$.

It is customary to study the spectra of isotopically substituted molecules in order to unambiguously identify the emitter of a particular band system, or confirm the vibrational and rotational analyses, perturbations etc. Though some experimental work has been done on certain electronic band systems of the isotopic molecules $^{13}C^{16}O$ and $^{12}C^{18}O$ the work done on the systems of $^{13}C^{18}O$ is very fragmentary. The Ångström bands of carbon monoxide present a rather interesting case in which perturbations are reported to have been caused in the $A\,^1\Pi$ state by more than one electronic state. These perturbations were studied in detail for the $^{12}C^{16}O$ molecule only. It is the aim of the present study to make use of the recently developed hollow cathode discharge tube of special design for the excitation of the Ångström band system of $^{13}C^{18}O$ and photograph them under high resolution. It is also the objective of this work to obtain a

better understanding of the nature of the perturbations by an analysis of the rotational structure of several bands of this system.

1.2 Previous Work on the $B\,^1\Sigma^+ - A\,^1\Pi$ Ångström Band System

The band system which is presently known as the Ångström system was first observed by Ångström and Thalén in 1875 and became known as the Second Positive system of carbon. Almost fifty years later, Birge (1926) analyzed this system and identified it as occurring from the allowed transition $B\,^1\Sigma^+ - A\,^1\Pi$ in $^{12}C\,^{16}O$ and named it after Ångström. This system has been the subject of numerous investigations for the reasons given earlier. Most of the earlier work was reviewed by Krupenie in 1966 in his monograph NSRDS - NBS 5 for the National Standard Reference Data Service of the National Bureau of Standards. Preliminary rotational analysis of the 0-1, 0-2, 0-3, and 1-1 bands of the Ångström system of $^{12}C\,^{16}O$ was attempted by Hulthén (1923) and Jasse (1926a,b) and they believed that the structure of the 0-0 and 1-0 bands was more complicated than the other bands of this system. More accurate work by Rosenthal and Jenkins (1929) and Schmid and Gerö (1935) revealed that the perturbations of the $A\,^1\Pi$ state of this system were the cause for the complicated structure of these bands and the resulting displacements of their heads from the expected positions. Johnson and Asundi (1929, 1936) reanalyzed the rotational structure of the 0-0 and 1-0 bands and also gave the fine structure analysis of the 0-4 and 0-5 bands. Coster and Brons (1934) have performed the rotational analysis of the 0-0, 0-1, 0-2, 0-3, and 0-4 bands to understand the perturbations of the $v = 0, 1, 2, 3$, and 4 levels of the $A\,^1\Pi$ state of $^{12}C\,^{16}O$. Schmid and Gerö (1935) obtained improved measurements of the rotational structure of the 0-0, 0-1, 1-0, and 1-1 bands and obtained the rotational

constants for the $B\,^1\Sigma^+$ state and the first vibrational separation $\Delta G(1/2)$.

McCulloh and Glockler (1953) photographed the Ångström band system of $^{13}C\,^{16}O$ molecule and have analyzed the fine structure of the 1-1, 0-1, 0-2, 0-3, 0-4, and 0-5 bands. Douglas and Møller (1955) have reanalyzed the 0-1, 1-1, and 0-2 bands of the Ångström system of $^{13}C\,^{16}O$ and examined the predissociations of the $^{12}C\,^{16}O$ and $^{13}C\,^{16}O$ molecules. Recently Rytel (1970a,b) and Kepa and Rytel (1970) have studied this system in $^{13}C\,^{16}O$, $^{12}C\,^{18}O$, and $^{12}C\,^{16}O$ under high resolution but no quantitative results on the perturbing states have been reported. The only preliminary report on the Ångström band system of $^{13}C\,^{18}O$ is given by Kepa *et al* (1972) who reported the band origins of the 0-1, 0-2, and 0-4 bands.

1.3 Present Investigation

Recently in our laboratory Bhogal (1982) excited the $^{13}C\,^{18}O$ molecules in a conventional electrodeless discharge tube using a microwave power generator and photographed the Ångström band system under medium dispersion and reported the isotope shifts of the band heads with respect to those of $^{12}C\,^{16}O$. For the present high resolution study, a hollow cathode discharge tube is used with a high voltage d.c. power supply to excite the $^{13}C\,^{18}O$ molecules. The rotational structure of all the intense Ångström bands, except the difficult 0-0 band, is analyzed. The rotational and the vibrational constants of both $B\,^1\Sigma^+$ and $A\,^1\Pi$ states are derived. The perturbations observed in the $A\,^1\Pi$ state are also studied quantitatively and the information about the perturbing states is obtained.

A description of the hollow cathode discharge tube and the details of the experimental techniques are presented in Chapter 2. In Chapter 3, the

rotational and the vibrational analyses of the intense bands along with the theory are presented. Interpretation of the perturbations observed in the $A\,^1\Pi$ state of $^{13}C\,^{18}O$ is given in Chapter 4.

CHAPTER 2

EXPERIMENTAL TECHNIQUES

The emission spectrum of $^{13}C^{18}O$ was excited in a hollow cathode discharge tube of special design and the resulting Ångström system was photographed with medium and high resolution optical spectrographs. A description of this hollow cathode tube and experimental procedure will be presented in this chapter.

2.1 Hollow Cathode Discharge Tube

The design of the hollow cathode discharge tube is schematically given in Fig.2. The cathode (G) is a copper hollow cylinder 19 mm in outer diameter and 90 mm long with a wall of thickness 4 mm. It is silver soldered (I) to a 19 mm inner diameter Kovar tube (H) which forms the lower portion of a 44 mm diameter Pyrex glass body (E) of the discharge tube. The bottom of the cathode is connected to a thin copper tubing (J). If required, any foreign gas can be passed into the discharge tube through J. For certain excitations, the hollow cathode tube can be immersed in liquid nitrogen (77K). In the present work, Ångström bands of $^{13}C^{18}O$ were excited in the tube without cooling or admission of a foreign gas. To the main body of the tube is attached a side branch (F) made of Pyrex glass 12 mm in diameter in which a tungsten anode (B) is fused. A ball and socket arrangement (A) is also provided as shown. Quartz windows (C and D), 3 mm in thickness, are attached to the anode and cathode branches of

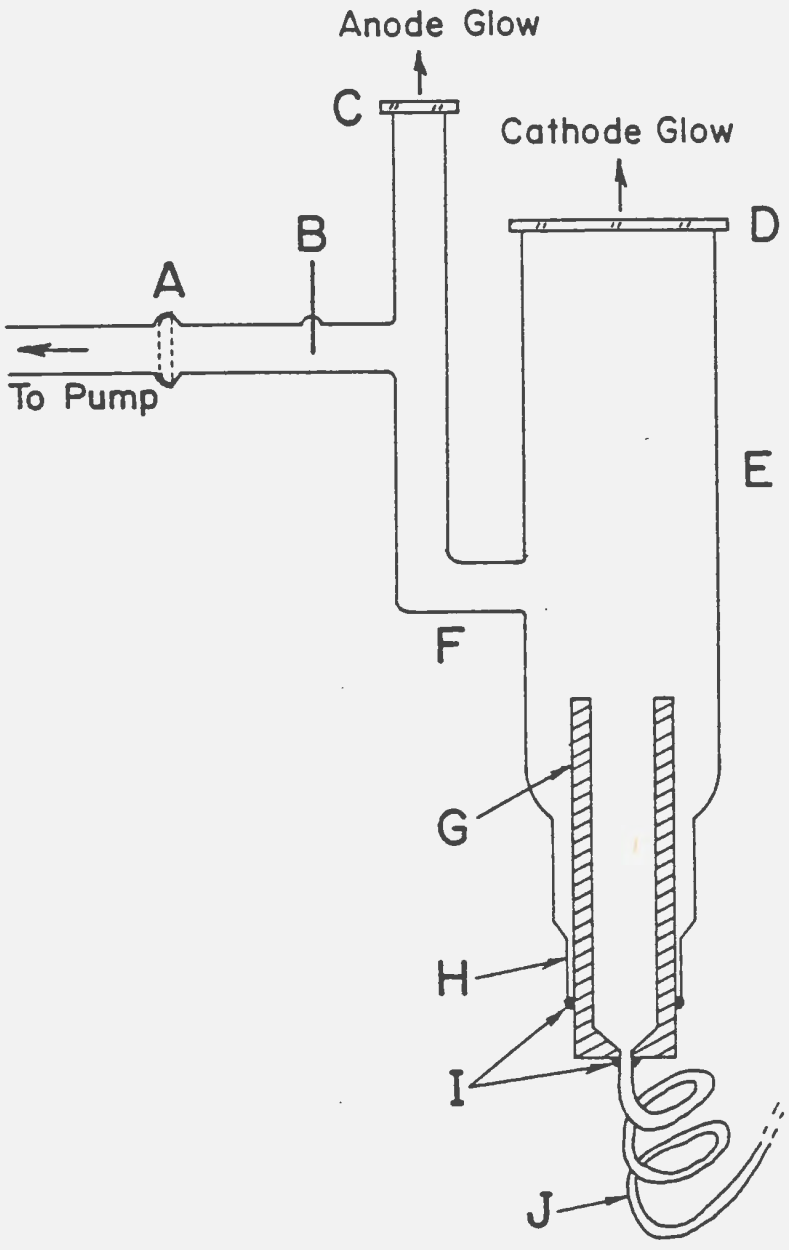

Fig. 2. A schematic diagram of the hollow cathode discharge tube : A: Ball and socket arrangement; B: Tungsten anode; C: Anode window; D: Cathode window; E: Pyrex glass body; F: Anode column; G: Copper cathode; H: Kovar glass - metal joint; I: Silver solderings; and J: Copper tubing.

the discharge tube respectively, with Torr Seal, a low vapor pressure resin. The present design of the hollow cathode discharge tube, which is somewhat similar to the one used by Herzberg *et al* (1981) for the excitation of triatomic molecular species H_3 and D_3, facilitates the physical separation of the anode and cathode glows.

The preliminary experiments on this discharge tube proved that the cathode glow is an excellent source to study the ionic species of the neutral molecules and the anode glow is convenient to photograph the electronic emission spectra of the neutral molecules. In the present study, the light emitted from the anode glow of the $^{13}C^{18}O$ discharge was photographed. If the discharge tube is cooled in the liquid nitrogen it is necessary to keep it vertical, in which case the light from the windows is to be directed onto the collimating lens of the optics by using a front coated mirror inclined at 45°. But in the present experiment, the hollow cathode was held in a horizontal position.

2.2 Power Supply Unit for the Hollow Cathode Discharge Tube

A 2000 V and 0.25 A d.c. power supply is used to maintain the discharge in the hollow cathode tube. A detailed circuit diagram of this unit is given in Fig.3. It mainly consists of a powerstat (P), a step - up transformer T (1750 - 0 - 1750 V), a bridge rectifier made up of four high voltage diffused silicon rectifiers D_1 to D_4 (VARO VC40), several DALE HL100 type resistors R_1 to R_7 and an oil filled condenser C (15 μF, 2000 V). The ratings of the resistors are as follows :

R_1 : 100 Ω, 100 W ; R_2 : Variable 1 - 20 KΩ, 100 W

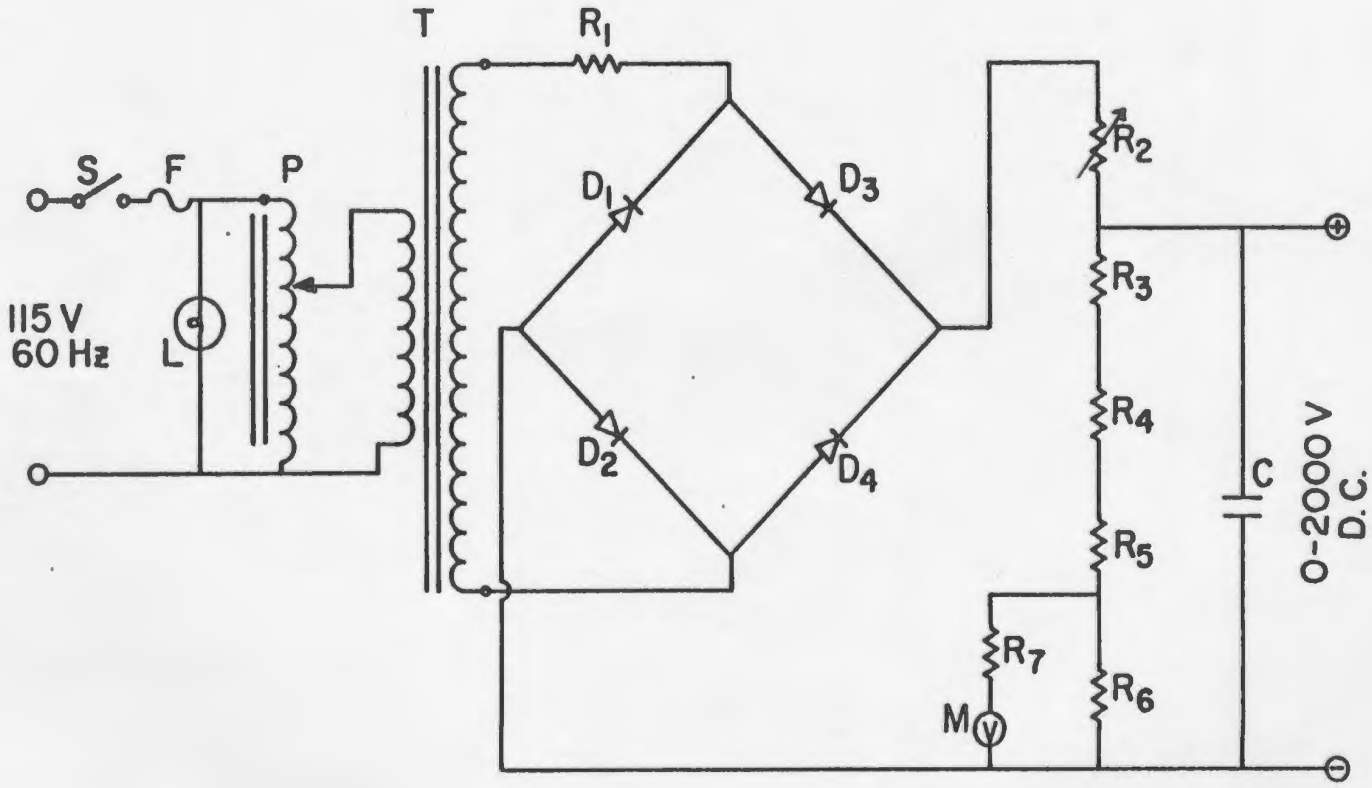

Fig. 3. Circuit diagram for the 2000 V d.c. power supply unit : P: Powerstat; T: Step - up transformer; D_1 to D_4: High voltage rectifiers; R_1 to R_7: Resistors; M: Voltmeter; and C: Oil-filled condenser.

R_3 to R_6 : 20 KΩ, 100 W ; and R_7 : 390 KΩ, 9 W

The primary voltage of the transformer is controlled through the powerstat. The output of the transformer is transferred to the bridge rectifier through R_1. The output of the bridge is fed to the bleeder resistors R_3 to R_6. As the current used in this power supply is less than 30 mA, R_2 is set at 20 KΩ and it acts as a bleeder resistor. The purpose of the bleeder resistor is to quickly discharge the capacitor when the unit is turned off. Voltmeter (M) measures the voltage across R_6. It was calibrated to 2500 V, according to the voltage on the capacitor, by means of R_7. The calibration was accurate up to 3%. By adjusting the powerstat, the required voltage can be applied across the electrodes of the discharge tube. As this power supply is operated at low currents, the characteristic spectrum of the experimental gas is normally obtained without any impurities.

2.3 Spectrographs

The emission spectrum of $^{13}C^{18}O$ was photographed with a 2 m Bausch and Lomb (B & L) dual grating spectrograph and a 3.4 m Jarrel - Ash (J - A) Ebert grating spectrograph. The optical layout of each of these instruments is briefly described in this section.

(i) The 2 m Bausch and Lomb Dual Grating Spectrograph

The optical layout of this spectrograph is schematically shown in Fig.4. Light from a source enters the spectrograph through the variable slit (S). It is then incident on the plane mirror (M) which reflects the light onto the upper section of the spherical mirror (SM) which has a focal length of 2 m and a numerical aperture of f/15.5. The collimated light from SM is then dispersed by one of the gratings G_1 or G_2. These gratings, one with 600

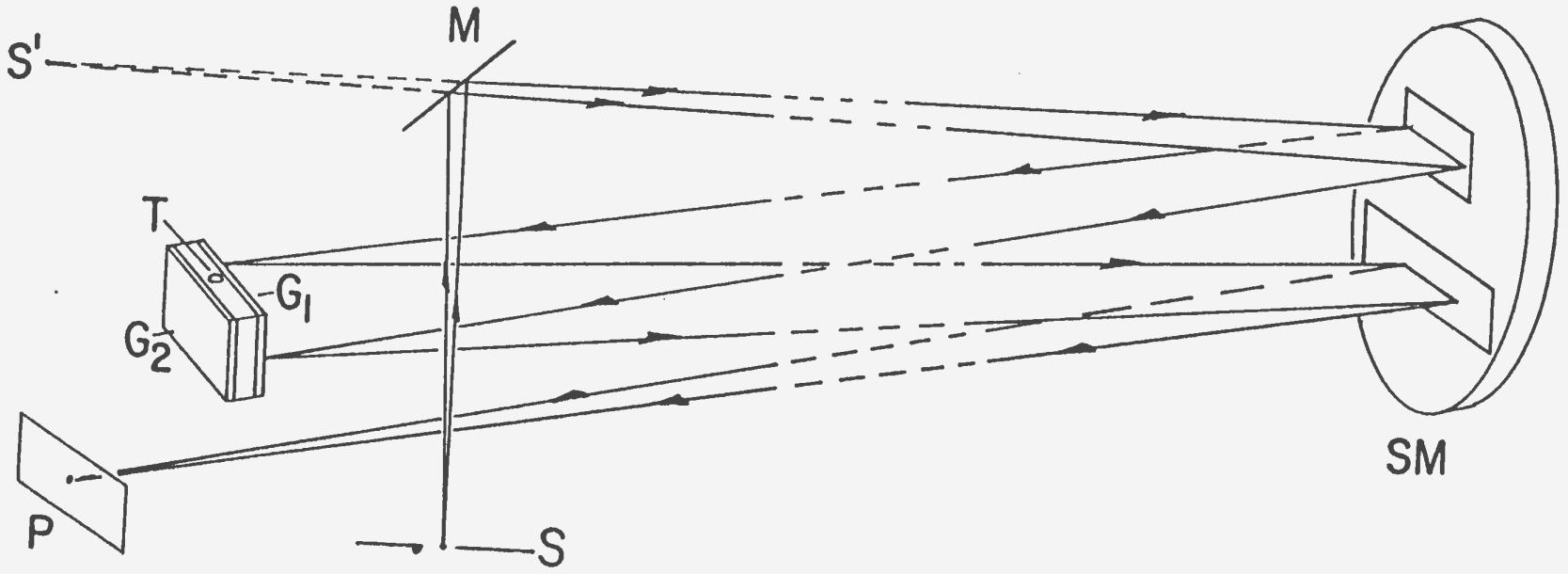

Fig. 4. Optical path of a monochromatic light beam in the 2 m Bausch and Lomb dual grating spectrograph : S: Slit; M: Plane mirror; SM: Spherical mirror; T: Rotatable turret; G_1 and G_2: Gratings; and P: Photographic plate.

grooves/mm and the other with 1200 grooves/mm and each having a ruled area of 102 mm × 128 mm, are mounted back to back on a rotatable turret (T). The required grating can be selected by rotating the turret. The dispersed light from the grating is then incident on the lower section of the spherical mirror which focuses it onto the photographic plate (P). The plate holder, designed to accommodate two 5.08 cm × 25.4 cm or one 10.16 cm × 25.4 cm plates, can be raised or lowered either manually or automatically. Located in front of the slit on the spectrograph is a Hartman diaphragm which provides a means of photographing the spectra in juxtaposition. The optical path shown in Fig.4. is for a monochromatic light. When polychromatic light enters the spectrograph, it is dispersed into the composite wavelengths which finally arrive at different positions on the photographic plate after collimation by the spherical mirror. The blaze wavelengths of the 600 and 1200 grooves/mm gratings are 2.5 and 1.0 μm respectively. The measured dispersions of the spectra are 8.2 Å/mm at 5500 Å in the first order of the 600 grooves/mm grating and 0.9 Å/mm at 4500 Å in the third order of the 1200 grooves/mm grating.

(ii) *The 3.4 m Jarrel - Ash Ebert Grating Spectrograph*

A schematic diagram of the optical arrangement of this spectrograph is shown in Fig.5. Light from a source after passing through two quartz lenses L_1 (focal length 10 cm and diameter 3 cm) and L_2 (focal length 45 cm and diameter 3 cm) enters the spectrograph through the slit (S). It is then incident on the upper section of the concave mirror (M) having a diameter of 40.6 cm, a radius of curvature of 6.655 m and a numerical aperture of f/35. The mirror (M) collimates the light onto the grating (G). The light dispersed by the grating consists of a parallel group of rays for

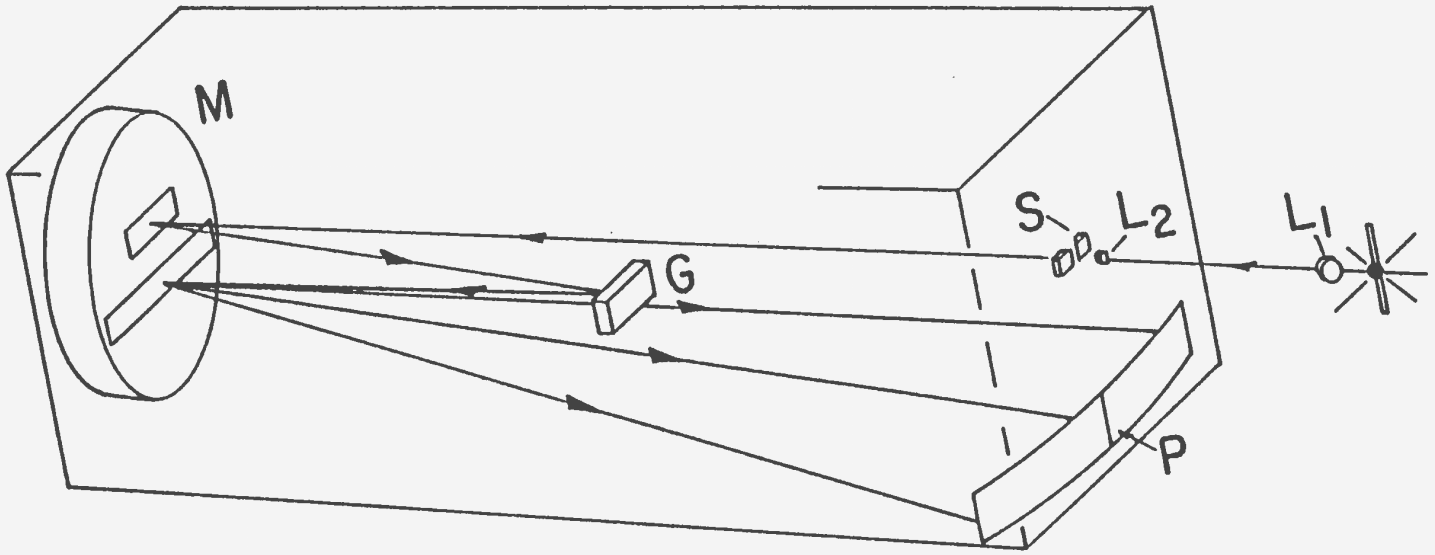

Fig. 5. Optical layout of the 3.4 m Jarrell - Ash Ebert grating spectrograph : L_1: Quartz cylindrical source lens, f=10.0 cm; L_2: Quartz cylindrical slit lens, f=45.0 cm; S: Entrance slit; M: Collimating mirror, diameter 40.6 cm; radius of curvature 6.658 m; G: Grating; and P: Photographic plate.

each wavelength and is collimated by the lower section of M onto the photographic plates (P). The camera which holds the plates can be tilted about a vertical axis. For a fixed slit position obtained for the best focus condition, the tilt of the camera is found to have a linear dependence on the grating angle. A typical plot of camera tilt versus the grating angle is given in Fig.6.

The spectrograph can be equipped with either an MIT echelle grating blazed at 5.7 μm and having 300 grooves/mm or a Bausch and Lomb plane grating blazed at 1.4 μm and having 1200 grooves/mm. Both these gratings have a ruled width of 186 mm and a groove length of 63 mm. In the present work the Bausch and Lomb grating was used in the second and third orders. The measured dispersions of the spectra photographed on this instrument are 0.9 Å/mm at 5500 Å in the second order and 0.6 Å/mm at 4500 Å in the third order.

2.4 Mechanism of Electrical Discharges

Electrical discharge in a discharge tube is produced essentially by three processes. Free electrons in an evacuated discharge tube are initially accelerated by an electrical field produced from a device such as a d.c. or a.c. power supply unit or a microwave generator. The translational kinetic energy of the electrons thus acquired is transferred, in a collision process, to the atoms and/or molecules in the discharge tube. In this process the atoms are excited to different higher electronic states and the molecules to their higher electronic, vibrational, and rotational states. Since these higher states of atoms and molecules are unstable, the excited atoms and/or molecules drop into their lower states through the emission of electromag-

Fig. 6. A plot of the camera tilt versus grating angle.

Fig. 6.

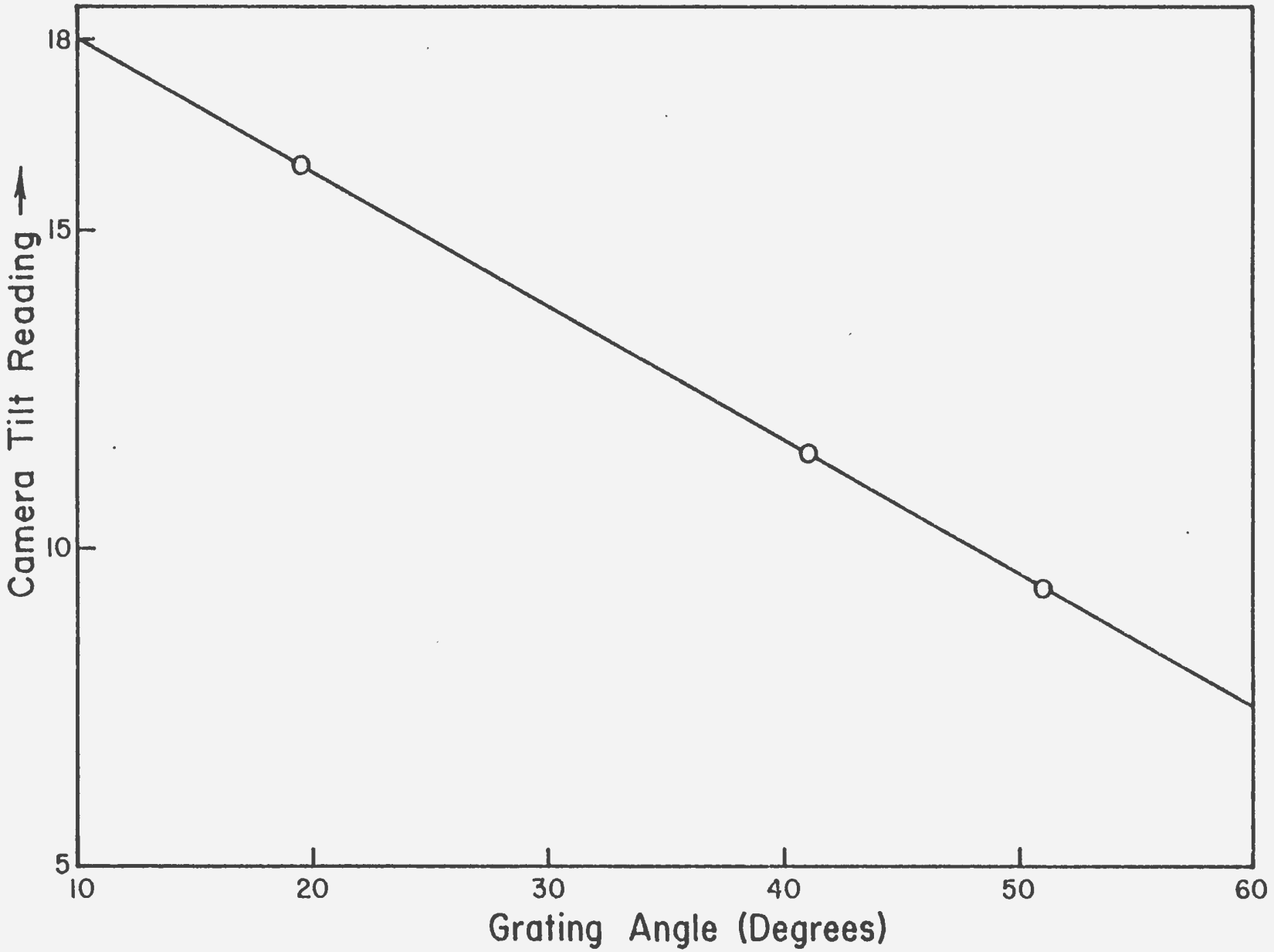
18
15
10
5
Camera Tilt Reading →
10
20
30
40
50
60
Grating Angle (Degrees)

netic radiation. The emitted radiation has energy $h\nu'$ (h being the Planck's constant and ν' being the frequency) which is equal to the energy difference between the upper and lower states. As long as the discharge tube is subjected to the electric field, collisions between the accelerated electrons and the atoms and/or molecules continue to take place and the emission of radiation is maintained.

2.5 Experimental Procedure

The $^{13}C^{18}O$ gas whose purity was given as 90.9% of ^{13}C atoms and 96.6% of ^{18}O atoms was supplied by Merck Sharpe and Dohme Canada Limited. The gas - handling system made of Pyrex glass which was attached to the hollow cathode discharge tube (Sec 2.1), is schematically shown in Fig.7. In this figure, R_1 and R_2 are the primary and secondary reservoirs respectively, S_1, S_2, and S_3 are stop-cocks, B is the ball and socket joint, and T is the liquid nitrogen trap. After thorough evacuation of the system up to S_1, the gas from R_1 was admitted into the discharge tube in stages through R_2 at required pressures. A d.c. voltage of 1200 V from the high voltage power supply (Sec 2.2) was applied between the two electrodes of the hollow cathode tube. A tesla coil was used to initiate the discharge. The pressure inside the discharge tube was regulated until a characteristic bright striations were observed in the anode column of the discharge tube. A steady discharge could be maintained for about 20 minutes, after which a fresh supply of $^{13}C^{18}O$ had to be readmitted to maintain the characteristic glow.

The anode branch of the hollow cathode discharge tube was optically aligned with the slit of the spectrograph. The Ångström band system of

Fig. 7. Gas handling system .: R_1 and R_2: Primary and secondary reservoirs; S_1, S_2, and S_3: Stop - cocks; B: Ball and socket arrangement; and T: Liquid nitrogen trap.

Fig. 7.

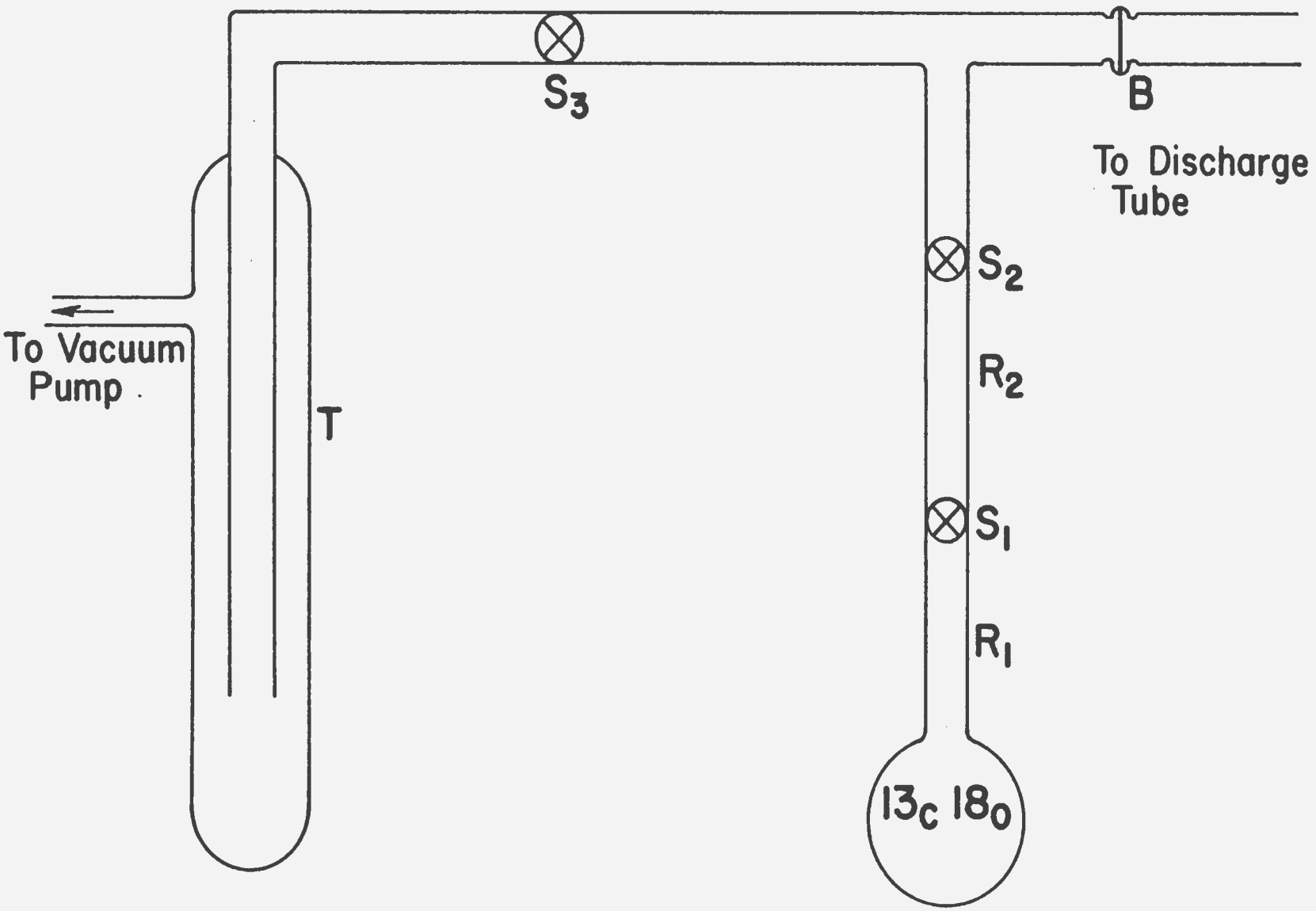
S3
B
To Discharge Tube
S2
To Vacuum Pump
T
R2
S1
R1
13C 18O

$^{13}C\,^{18}O$ was photographed in the first order with a 600 grooves/mm grating on the 2 m B & L spectrograph. Using the 1200 grooves/mm grating on this spectrograph the 1-1, 0-0, and 0-1 bands were photographed in the third order and the 0-4 and 0-5 bands were photographed in the second order. The 3.4 m J - A spectrograph equipped with a Bausch and Lomb 1200 grooves/mm grating was used to photograph the 1-0 band in the third order and the 0-2 and 0-3 bands in the second order. Kodak Spectrum Analysis No.1, 103 a-o, Tri-x Panchromatic type B and 103-F plates were used to photograph the bands and the Corning glass filters were used to eliminate the overlapping higher orders. The slit width was maintained at 20 μm and 30 μm on the B & L and J - A spectrographs respectively. Depending on the intensity of the band, sensitivity of the photographic plate, and transmittance of the filter the exposure times varied from 10 to 75 minutes on the B & L spectrograph and 30 min. to 2 hours on the J - A spectrograph. Iron arc and Fe - Ne hollow cathode lamp were used as sources of standard spectra.

All the photographic plates were developed in Kodak developer D-19 for 4 to 5 minutes. After rinsing them in cold water, they were fixed in the Kodak fixer kept at 20°C for about 5 to 15 minutes. The plates were dried after washing them in running water for 30 minutes.

2.6 Measurement of Spectra

The photographic plates were measured on a linear comparator model M 1205 C supplied by the Gaertner Optical Company, Chicago, Illinois, U.S.A. The least count of the instrument is 0.001 mm but the readings could be estimated to 0.0001 mm. The comparator readings (d) were

obtained for the band heads, rotational lines, and standard lines. The air wavelengths λ_{air} of the standard lines and their corresponding comparator readings (d) were fitted to the polynomial

$$\lambda_{air} = \sum_{i=0}^{i=n} a_i \, (d - d_0)^i, \qquad (2.1)$$

and the coefficients a_0, a_1, a_2,.....etc., were obtained by the method of least squares. In Eq.(2.1), d_0 is the position of the first standard line. In general, the third degree polynomial was found to be adequate for a satisfactory fit. The accuracy, of the coefficients obtained from the polynomial least squares fit, was tested by calculating the wavelengths of the some standard lines in the same region. In general, the accuracy of the measurements was ~0.0005 Å in the third order and 0.003 Å in the first order, but somewhat less for diffused lines.

The air wavelengths of the band heads and the rotational lines were calculated using the Eq.(2.1). These were converted into vacuum wavenumbers ν (cm^{-1}) by using the Edlen's formula for the refractive index, n,

$$n = 1 + 6432.8 \times 10^{-8} + \frac{2949810}{146 \times 10^8 - \nu^2} + \frac{25540}{41 \times 10^8 - \nu^2} \qquad (2.2)$$

where $\nu = \frac{10^8}{n \times \lambda_{air}}$, ($\lambda_{air}$ in Ångström units).

An iterative method was employed to calculate the vacuum wavenumbers and the iteration was continued until the absolute value of the difference between the successive values of the wavenumbers was less than or equal to 10^{-10} cm^{-1}. The mathematical calculations involved were performed on an IBM 370 computer and also on the Hewlett-Packard calculator model 9825A.

CHAPTER 3

VIBRATIONAL AND ROTATIONAL STRUCTURE OF THE ÅNGSTRÖM BAND SYSTEM OF $^{13}C^{18}O$

In this chapter, the vibrational and rotational analyses of the $B\,^1\Sigma^+ - A\,^1\Pi$ Ångström bands of $^{13}C^{18}O$ will be given. The theory pertinent to the $^1\Sigma^+ - {}^1\Pi$ electronic transition will be outlined briefly in Sec.3.1. The spectrograms of the band heads photographed under medium dispersion and the assignment of the vibrational quantum numbers will be given in Sec.3.2. In sec.3.3, high resolution spectrograms and the details of the rotational analysis of several bands will be presented. Finally, the vibrational analysis performed with the band origins will be given in Sec.3.4.

3.1 Theory

(i) The vibrational and rotational terms

The total energy E (usually expressed in ergs) of a diatomic molecule, neglecting its translational and nuclear spin energies, can be represented within the Born - Oppenheimer approximation as the sum of its electronic energy E_e, the vibrational energy E_v, and the rotational energy E_r, i.e.,

$$E = E_e + E_v + E_r. \qquad (3.1)$$

The term value T (in cm^{-1}) of a particular energy level is represented as

$$T = \frac{E}{hc} = T_e + G(v) + F_v(J), \qquad (3.2)$$

where v and J are the vibrational and rotational quantum numbers respectively, and T_e, G(v) and $F_v(J)$ are the electronic, vibrational, and rotational term values respectively. The vibrational term values G(v) in an electronic state of a molecule are expressed as

$$G(v) = \omega_e(v + 1/2) - \omega_e x_e (v + 1/2)^2 + \omega_e y_e (v + 1/2)^3 + \ldots\ldots \quad (3.3)$$

where ω_e is the vibrational frequency (in cm^{-1}) and $\omega_e x_e$, $\omega_e y_e$, ... are the anharmonic terms of the vibrational motion. The rotational term values belonging to a given vibrational level of a singlet electronic state (for which the resultant electronic spin S is zero) are represented by

$$F_v(J) = B_v J(J + 1) - D_v J^2 (J + 1)^2 + \ldots\ldots \quad (3.4)$$

where $B_v = \left[\frac{h}{8\Pi^2 c \mu}\right] \left[\frac{1}{r^2}\right]$ is the rotational constant (μ is the reduced mass of the molecule and r is the internuclear distance) and $D_v = \frac{4B_v^3}{\omega^2}$ is the centrifugal stretching constant. B_v and D_v are represented in terms of the vibrational quantum number as

$$B_v = B_e - \alpha_e(v + 1/2) + \gamma_e(v + 1/2)^2 + \ldots\ldots \quad (3.5)$$

and

$$D_v = D_e + \beta_e(v + 1/2) + \ldots\ldots$$

where

$$B_e = \frac{h}{8\Pi^2 c \mu r_e^2} \quad \text{and} \quad D_e = \frac{4B_e^3}{\omega_e^2} \quad (3.6)$$

are the constants corresponding to the equilibrium internuclear separation r_e. In Eq.(3.5), $\alpha_e \ll B_e$, $\gamma_e \ll \alpha_e$ and $\beta_e \ll D_e$.

(ii) The vibrational structure

The wavenumber (in cm^{-1}) of a spectral line arising from a transition between the rotational levels of two singlet electronic states is given by

$$\nu = (T_e' - T_e'') + (G'(v) - G''(v)) + (F_v'(J') - F_v''(J'')) \quad (3.7)$$

$$= \nu_e + \nu_v + \nu_r. \quad (3.8)$$

For a given electronic transition ν_e is the **system origin** and $(\nu_e + \nu_v)$ is the **band origin** . Neglecting cubic and higher order terms in Eq.(3.3), the band origin of a band system can be written as

$$\nu_0 = \nu_e + \omega_e'(v' + 1/2) - \omega_e'x_e'(v' + 1/2)^2 - [\omega_e''(v'' + 1/2) - \omega_e''x_e''(v'' + 1/2)^2] \quad (3.9)$$

The vibrational quanta $\Delta G(v + 1/2)$ between the vibrational levels v and v+1 of a given electronic state are represented by

$$\Delta G(v + 1/2) = (\omega_e - \omega_e x_e) - 2\omega_e x_e (v + 1/2) \quad (3.10)$$

and the second differences are given by

$$\Delta^2 G(v + 1) = \Delta G(v + 3/2) - \Delta G(v + 1/2) \quad (3.11)$$

$$= -2\,\omega_e x_e$$

(iii) The rotational structure

If one of the electronic states of a transition has $\Lambda \neq 0$ (Λ is the quantized projection of the electronic orbital angular momentum along the internuclear axis), the rotational selection rules for the electric dipole radiation are

$\Delta J = 0, \pm 1$; $J = 0 \not\longleftrightarrow J = 0$, $+ \longleftrightarrow -$; $+ \not\longleftrightarrow +$, $- \not\longleftrightarrow -$.

Branches corresponding to $\Delta J = -1, 0,$ and $+1$ are named as P, Q, and R respectively. The wavenumbers of the spectral lines in P, Q, and R branches are given by the expressions

$$P(J) = \nu_0 + F'_v(J-1) - F''_v(J) \quad (3.12)$$

$$Q(J) = \nu_0 + F'_v(J) - F''_v(J) \quad (3.13)$$

$$R(J) = \nu_0 + F'_v(J+1) - F''_v(J) \quad (3.14)$$

where ν_0 is the band origin and J is the rotational quantum number of the lower state. On substitution of Eq.(3.4) for F_v (J)'s in Eqs.(3.12, 13, and 14)

$$P(J) = \nu_0 - (B'_v + B''_v)J + (B'_v - B''_v - D'_v + D''_v)J^2 + 2(D'_v + D''_v)J^3 - (D'_v - D''_v)J^4 \quad (3.15)$$

$$Q(J) = \nu_0 + (B'_v - B''_v)J + (B'_v - B''_v - D'_v + D''_v)J^2 - 2(D'_v - D''_v)J^3 - (D'_v - D''_v)J^4 \quad (3.16)$$

$$R(J) = \nu_0 + (2B'_v - 4D'_v) + (3B'_v - B''_v - 12D'_v)J + (B'_v - B''_v - 13D'_v + D''_v)J^2 - 2(3D'_v + D''_v)J^3 - (D'_v - D''_v)J^4 \quad (3.17)$$

For bands with Q-branches the combination relations are written as

$$R(J) - Q(J) = F'_v(J+1) - F'_v(J) = \Delta_1 F'_v(J) \quad (3.18)$$

$$Q(J+1) - P(J+1) = F'_v(J+1) - F'_v(J) = \Delta_1 F'_v(J) \quad (3.19)$$

$$R(J) - Q(J+1) = F''_v(J+1) - F''_v(J) = \Delta_1 F''_v(J) \quad (3.20)$$

$$Q(J) - P(J+1) = F''_v(J+1) - F''_v(J) = \Delta_1 F''_v(J) \quad (3.21)$$

Eqs.(3.18 and 19) give the upper state combination differences whereas Eqs. (3.20 and 21) give the lower state combination differences. The second differences which can be used to obtain the rotational constants of the lower and the upper states are written as

$$\Delta_2 F_v(J) = 4B_v(J + 1/2) - 8D_v(J + 1/2)^3 \quad (3.22)$$

where

$$\Delta_2 F''_v(J) = R(J-1) - P(J+1)$$

and

$$\Delta_2 F'_v(J) = R(J) - P(J)$$

The P, Q, and R branches occurring in a $^1\Sigma^+ - {}^1\Pi$ transition are schematically shown in Fig.8.

3.2 Assignment of Vibrational Quantum Numbers for the Band Heads

As mentioned in Chapter 2, the Ångström bands of $^{13}C^{18}O$ were excited in a hollow cathode discharge tube. Altogether eight characteristic sharp bands have been observed in the spectral region 4100 - 6500 Å. Because of the impurities present in the sample of $^{13}C^{18}O$, several Ångström bands of $^{13}C^{16}O$ and $^{12}C^{16}O$ have also been observed in the same region. The spectrum photographed under medium dispersion in the first order of 600 grooves/mm grating on the 2 m B & L spectrograph is reproduced in Fig.9. Due to the simple vibrational structure of the $^{13}C^{18}O$ bands and the presence of the known Ångström bands of the $^{12}C^{16}O$ and $^{13}C^{16}O$ molecules, the assignment of the vibrational quantum numbers to the $^{13}C^{18}O$ bands was found to be straightforward. The vacuum wavenumbers (in cm^{-1}) of the band heads of $^{13}C^{18}O$, their relative intensities, and vibrational quantum numbers are listed in Table.1. In principle, the vibrational constants for the A and B states can be obtained from the band head data. However, the more accurate vibrational constants can be obtained from the band origin data. Hence the vibrational constants of the A and B states of $^{13}C^{18}O$ are obtained from the band origin data, derived from the detailed rotational analysis of the several bands of the Ångström

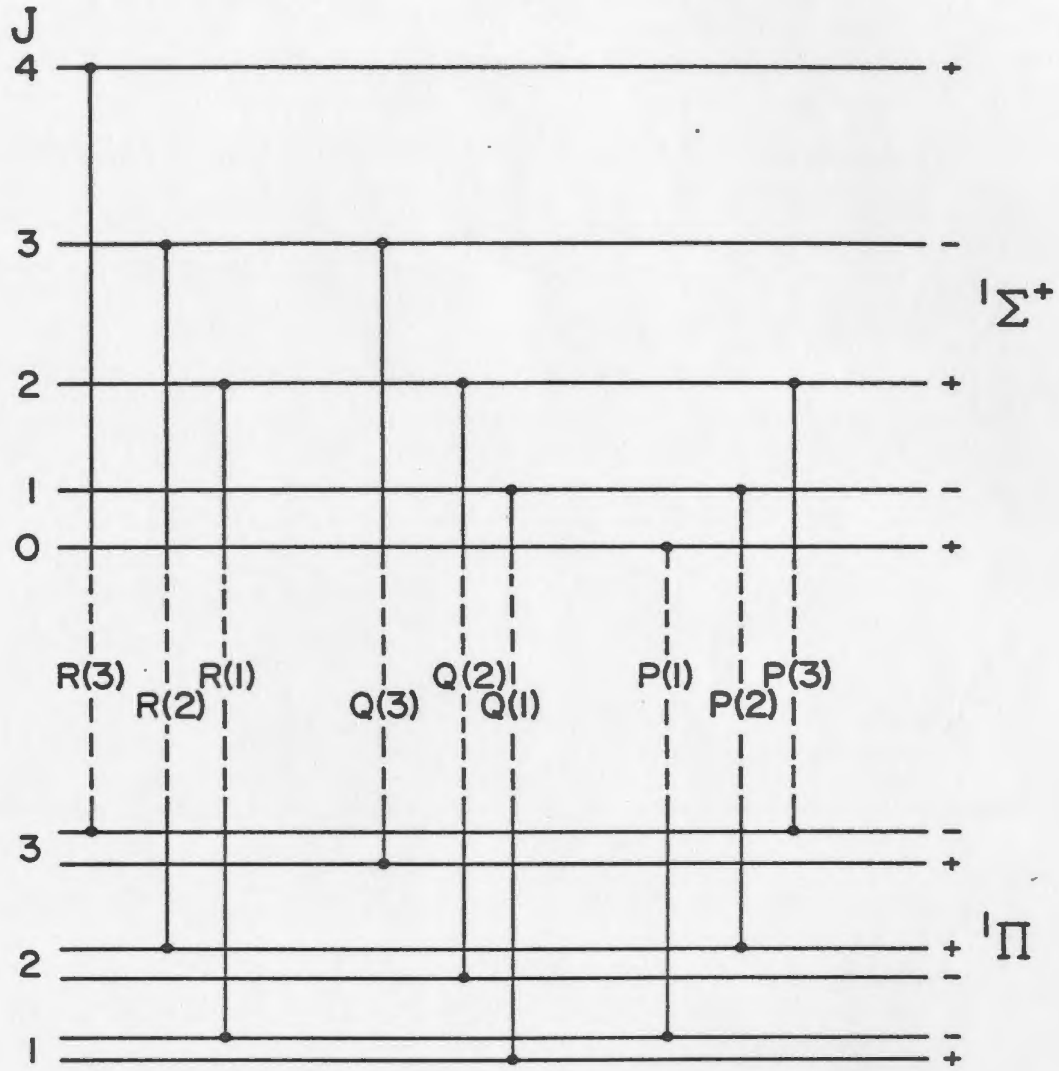

Fig. 8. A schematic energy level diagram showing the rotational transitions in a $^1\Sigma^+ - {}^1\Pi$ transition.

Fig. 9. The $B\,^1\Sigma^+ - A\,^1\Pi$ Ångström band system of $^{13}C^{18}O$ photographed under medium dispersion.

Fig. 9.

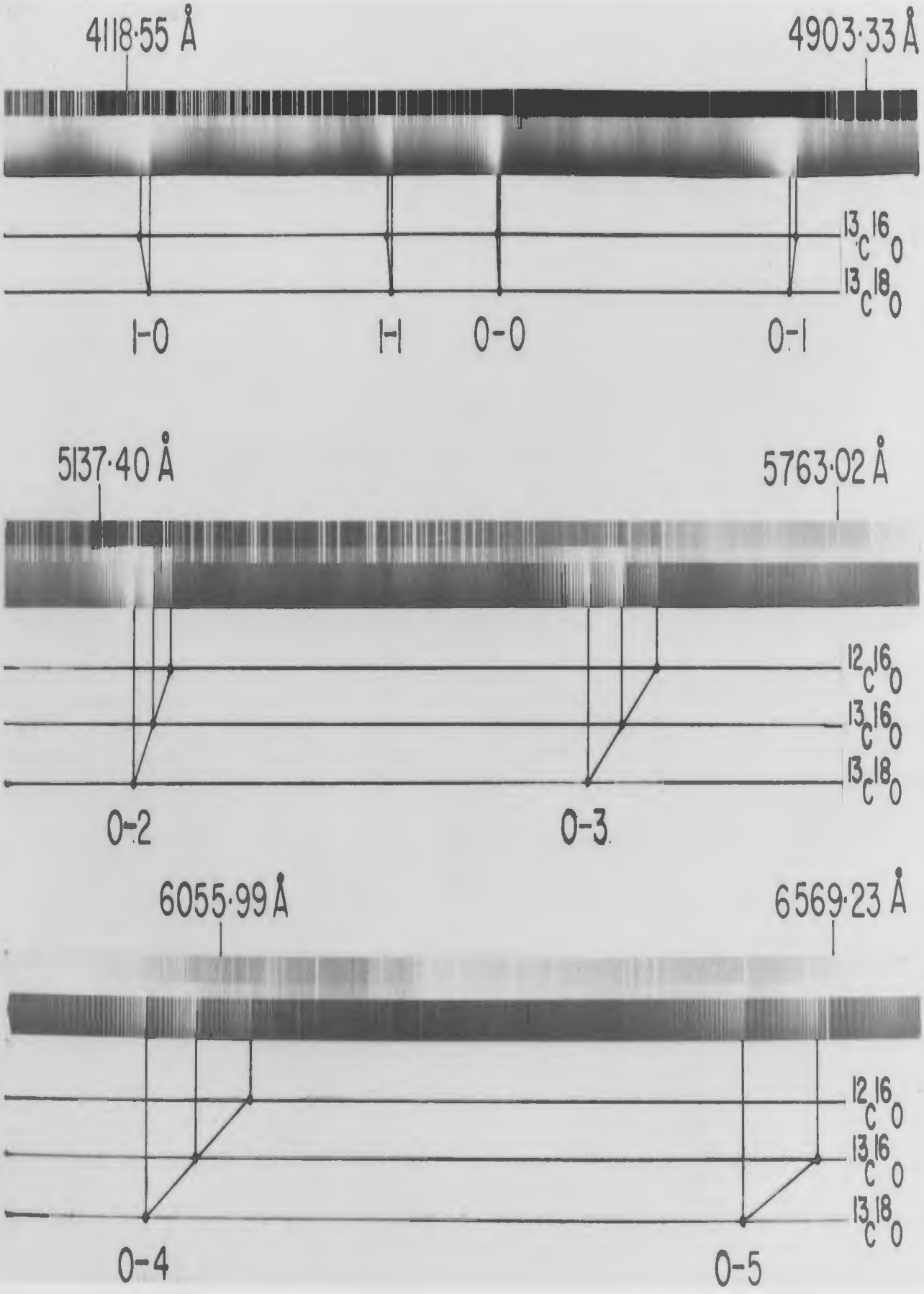
4118·55 Å
4903·33 Å
$^{13}C^{16}O$
$^{13}C^{18}O$
1-0
1-1
0-0
0-1
5137·40 Å
5763·02 Å
$^{12}C^{16}O$
$^{13}C^{16}O$
$^{13}C^{18}O$
0-2
0-3
6055·99 Å
6569·23 Å
$^{12}C^{16}O$
$^{13}C^{16}O$
$^{13}C^{18}O$
0-4
0-5

TABLE 1. Band heads of Ångström System of $^{13}C\,^{18}O$

Vacuum Wavenumber (cm^{-1})	Relative Intensity*	v'-v''
24127.58	s	1-0
22719.18	w	1-1
22142.58	vs	0-0
20732.27	vs	0-1
19351.01	m	0-2
18002.03	w	0-3
16682.68	w	0-4
15396.08	vw	0-5

* Abbreviations for relative intensities vs, s, m, w, and vw denote very strong, strong, medium, weak, and very weak respectively.

system in Sec.3.3. The arrangement of the band heads in the Deslandres scheme indicated that the 1-0, 0-0, and 0-3 bands were perturbed.

3.3 Rotational Analysis

High resolution spectra of all the eight bands of the Ångström system of $^{13}C^{18}O$ were photographed in the second and third orders of the B & L and the J - A spectrographs using the 1200 grooves/mm grating in each case. The details of the bands photographed are given below.

Band	Spectrograph	Order
1-0	J - A	Third
1-1	B & L	Third
0-0	B & L	Third
0-1	B & L	Third
0-2	J - A	Second
0-3	J - A	Second
0-4	B & L	Second
0-5	B & L	Second

A complete rotational analysis for the 1-1, 0-1, 0-2, 0-3, 0-4, and 0-5 bands and a partial analysis for the 1-0 band were carried out. However, no analysis was possible for the 0-0 band because of the severe perturbations in the v = 0 level of $A\,^1\Pi$ state and the overlap of the 0-0 bands of other isotopically substituted species of carbon monoxide.

The rotational structures of the 0-1, 0-2, 0-3, and 0-5 bands are shown in Figs.10, 11, 12, and 13 respectively. In the 0-1 band the R(1) line was too weak to observe. In the 0-2 and 0-4 bands there was a complete overlap of the R and P branches. Due to this overlap the combination differences in these two bands did not agree very well as they did in other bands. In the 0-3 band, the perturbations were observed at J=2, 6, and 10 in Q, P and R, and Q branches respectively and the detailed

Fig. 10. Rotational structure of the 0-1 band.

Fig. 10.

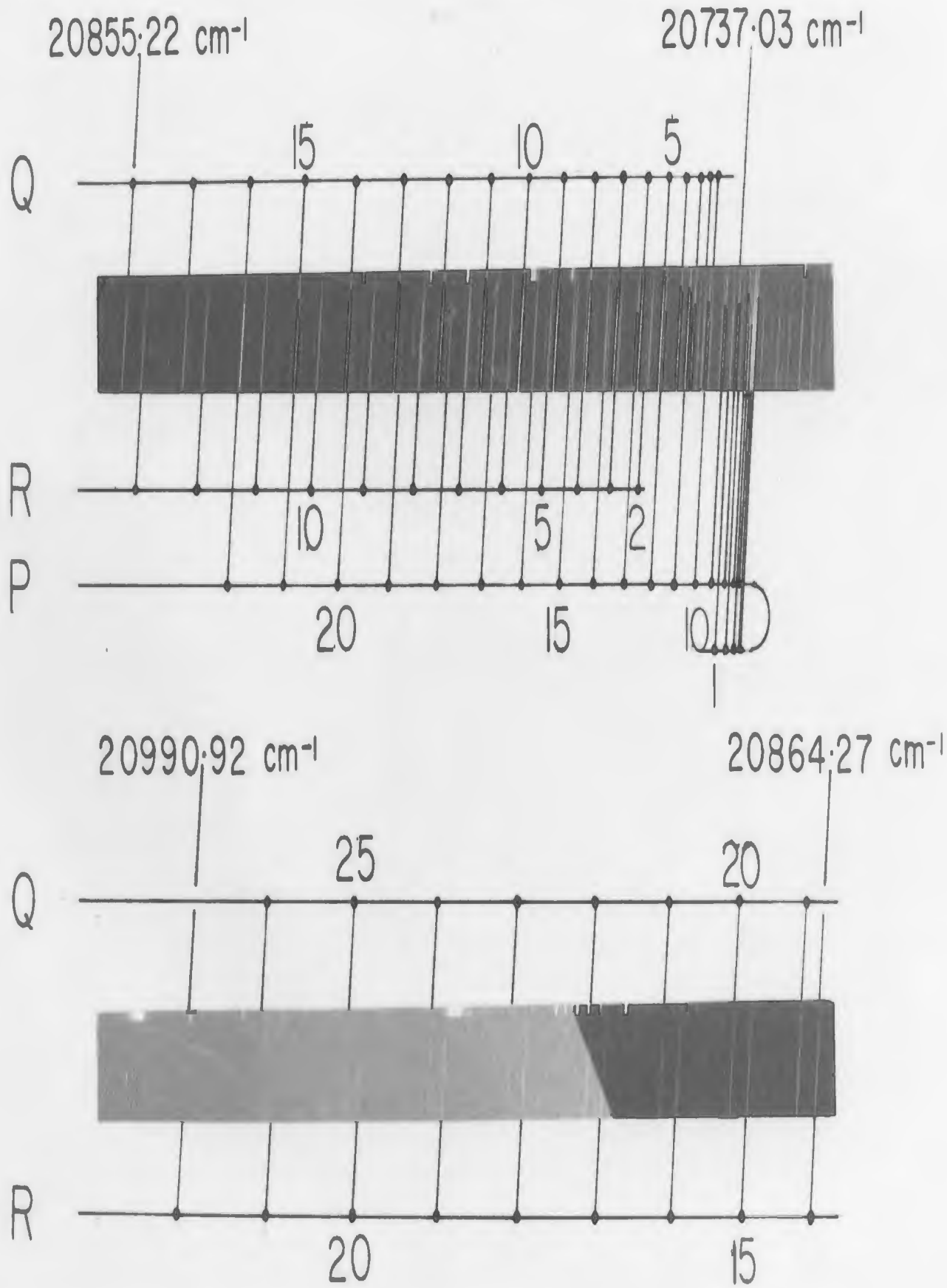
20855.22 cm-1
20737.03 cm-1
Q
15
10
5
R
10
5
2
P
20
15
10
1
20990.92 cm-1
20864.27 cm-1
Q
25
20
R
20
15

Fig. 11. Rotational structure of the 0-2 band.

Fig. 11.

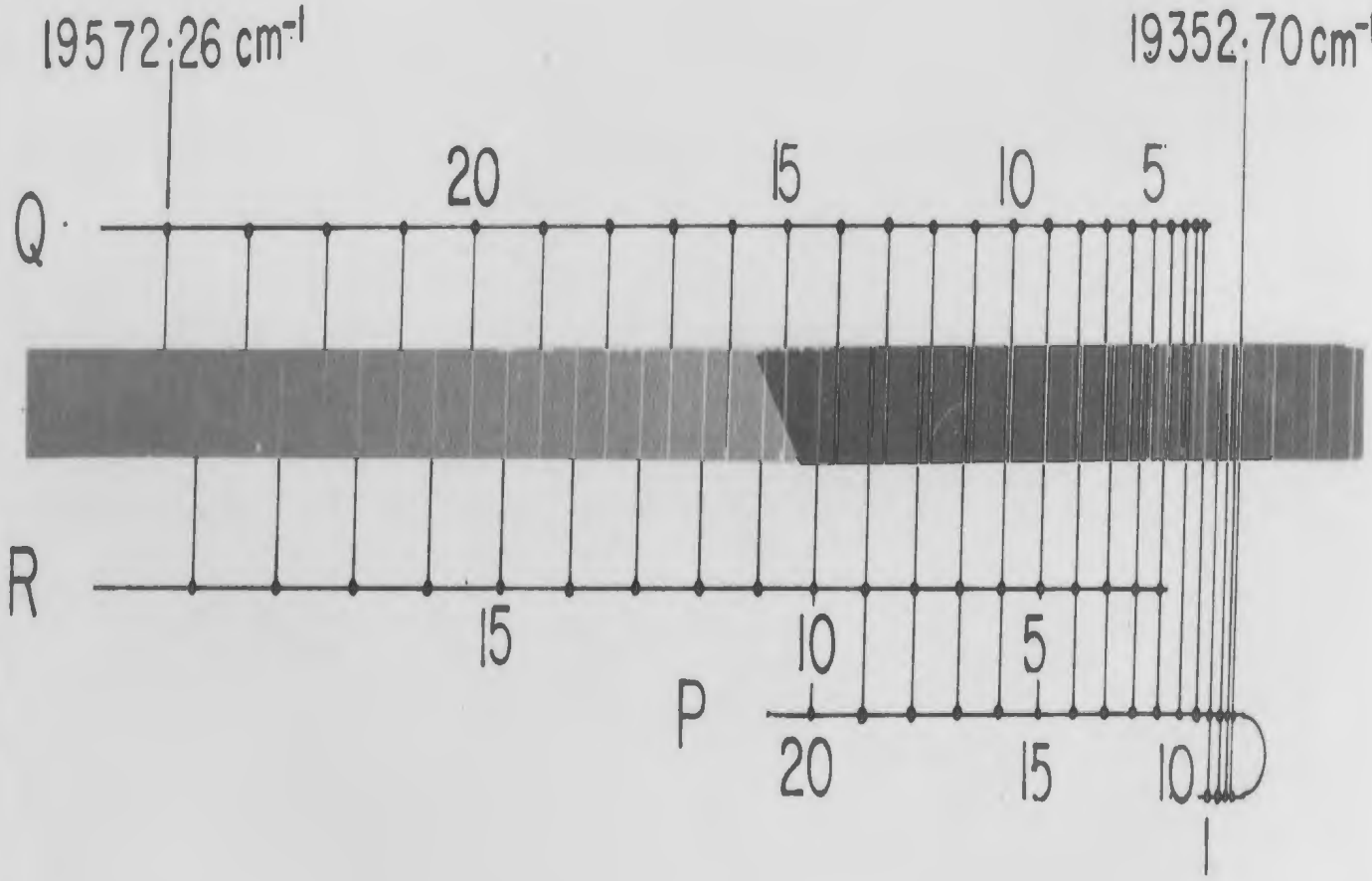
19572.26 cm⁻¹
19352.70 cm⁻¹
Q
20
15
10
5
R
15
10
5
P
20
15
10
1

Fig. 12. Rotational structure of the 0-3 band.

Fig. 12.

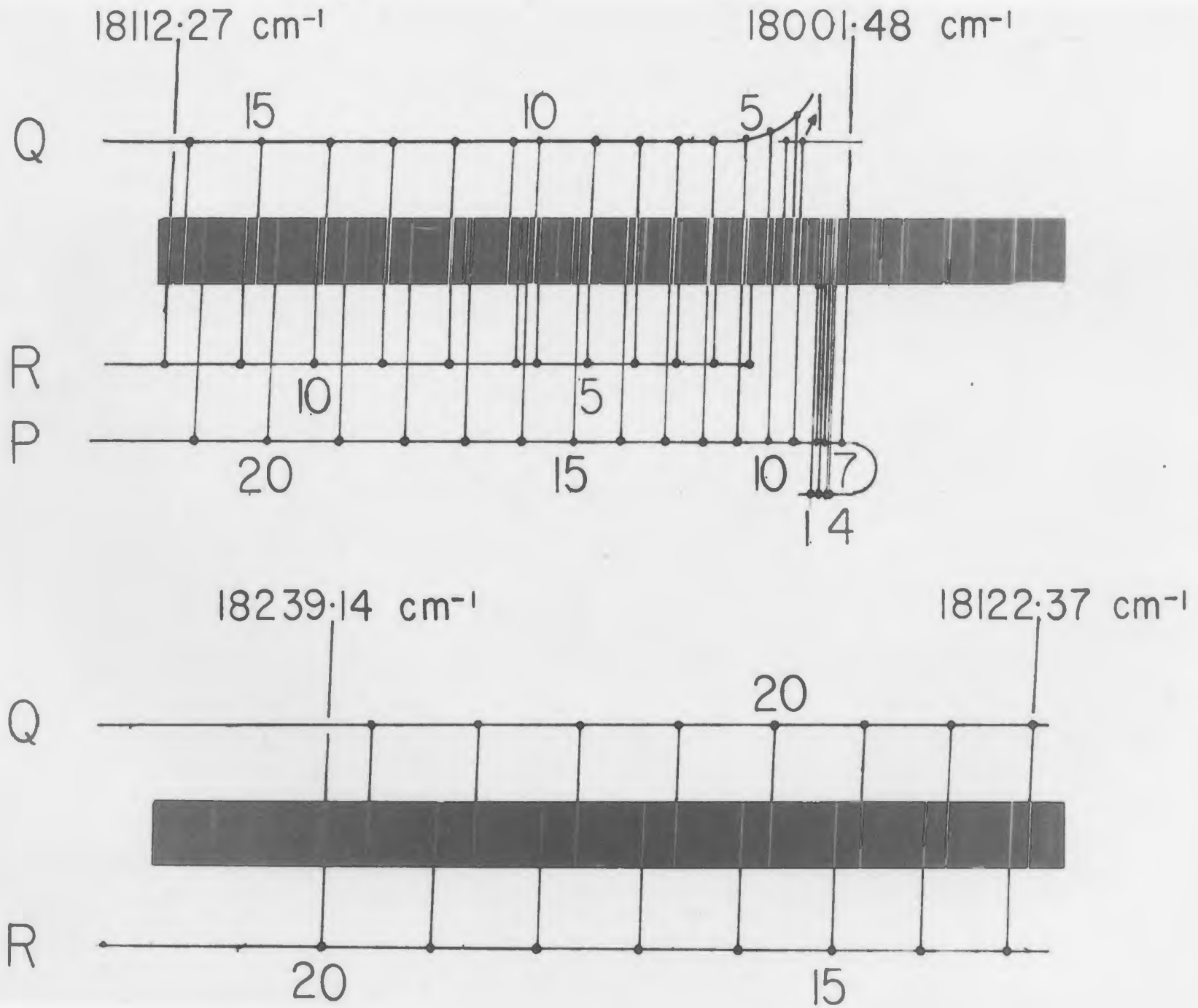
18112·27 cm⁻¹
18001·48 cm⁻¹
Q
15
10
5
1
R
10
5
P
20
15
10
7
1
4
18239·14 cm⁻¹
18122·37 cm⁻¹
Q
20
R
20
15

Fig. 13. Rotational structure of the 0-5 band.

Fig. 13.

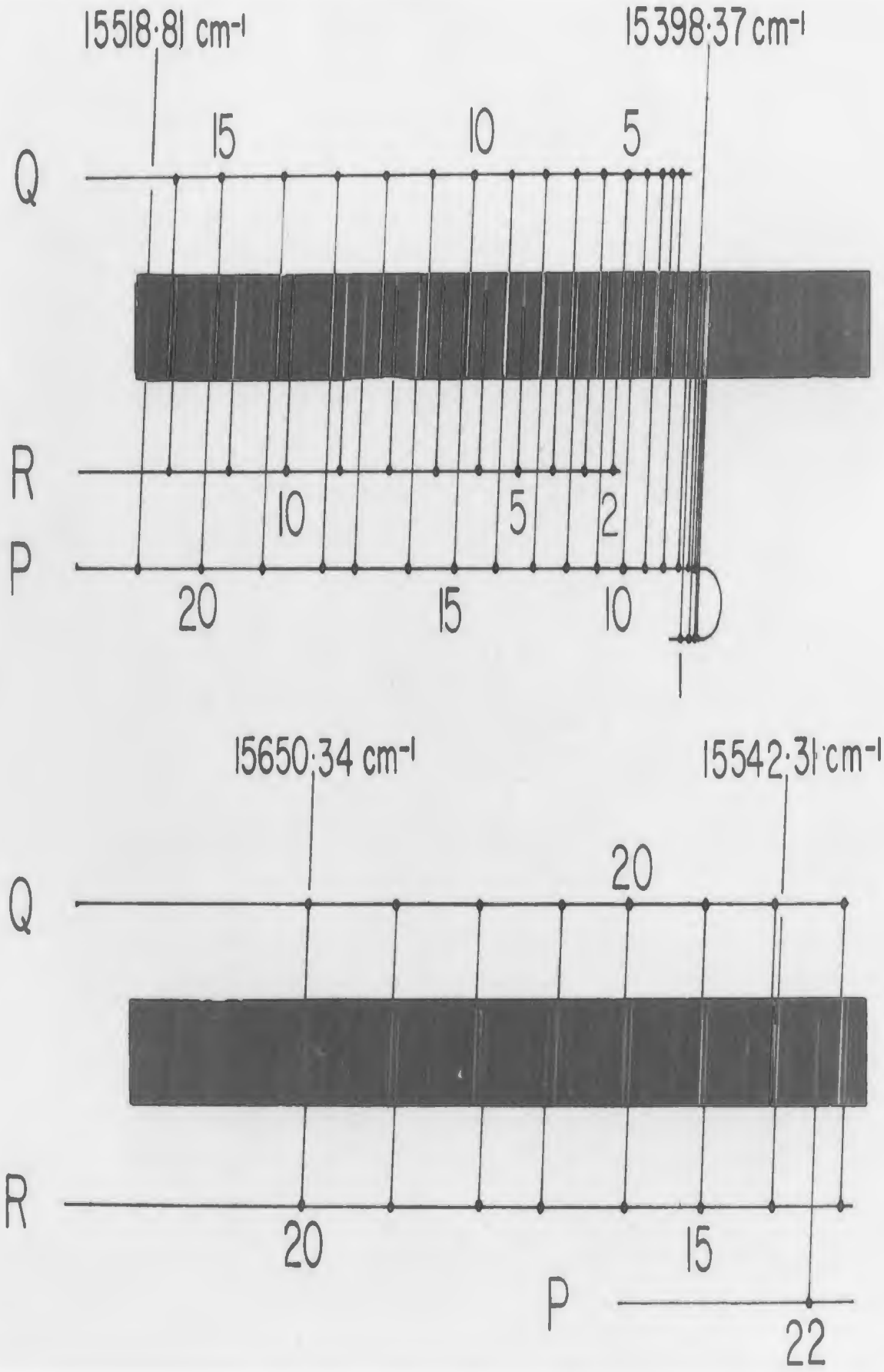
15518·81 cm⁻¹
15398·37 cm⁻¹
15
10
5
Q
R
P
10
5
2
20
15
10
1
15650·34 cm⁻¹
15542·31 cm⁻¹
20
Q
R
20
15
P
22

study of these perturbations showed that the band origin of this band was shifted due to these perturbations. In the 0-5 band, the perturbations were observed at J=15, 18, and 21 in Q, P and R, and Q branches respectively but no shift in the band origin was observed. In this band also the R(1) line was too weak to observe. In the 1-0 band, the perturbations were observed at J=7 and 10 in Q and P branches respectively. As some rotational lines, particularly near the head, were very weak, the rotational quantum numbers for these lines could not be assigned. The vacuum wavenumbers and J assignments of the rotational lines of the bands analyzed are given in Tables. 2 to 8.

The rotational constants of the lower ($A\,^1\Pi$) and the upper ($B\,^1\Sigma^+$) states were obtained from the combination relation

$$\frac{\Delta_2 F_v(J)}{J + 1/2} = 4B_v - 8D_v(J + 1/2)^2 \qquad (3.23)$$

The rotational constants B_v and D_v were determined by linear least squares fits of the quantities $\frac{\Delta_2 F_v(J)}{(J + 1/2)}$ against $(J + 1/2)^2$. As an example, the fit obtained for the 0-1 band is given in Fig.14. The values of B_0, B_1, D_0, and D_1 of the upper state and B_1, B_2, B_4, B_5, D_1, D_2, and D_5 are listed in Table.9.

If one neglects the stretching constants D'_v and D''_v the Q-branch lines can be represented by the relation

$$Q(J) = \nu_0 + (B'_v - B''_v)\,J(J + 1) \qquad (3.24)$$

The band origins ν_0 and the differences $(B'_v - B''_v)$ were obtained by the linear least squares fits of the wavenumbers Q(J) against J(J + 1). As an example, the fit obtained for the Q-branch lines of the 0-1 band is shown

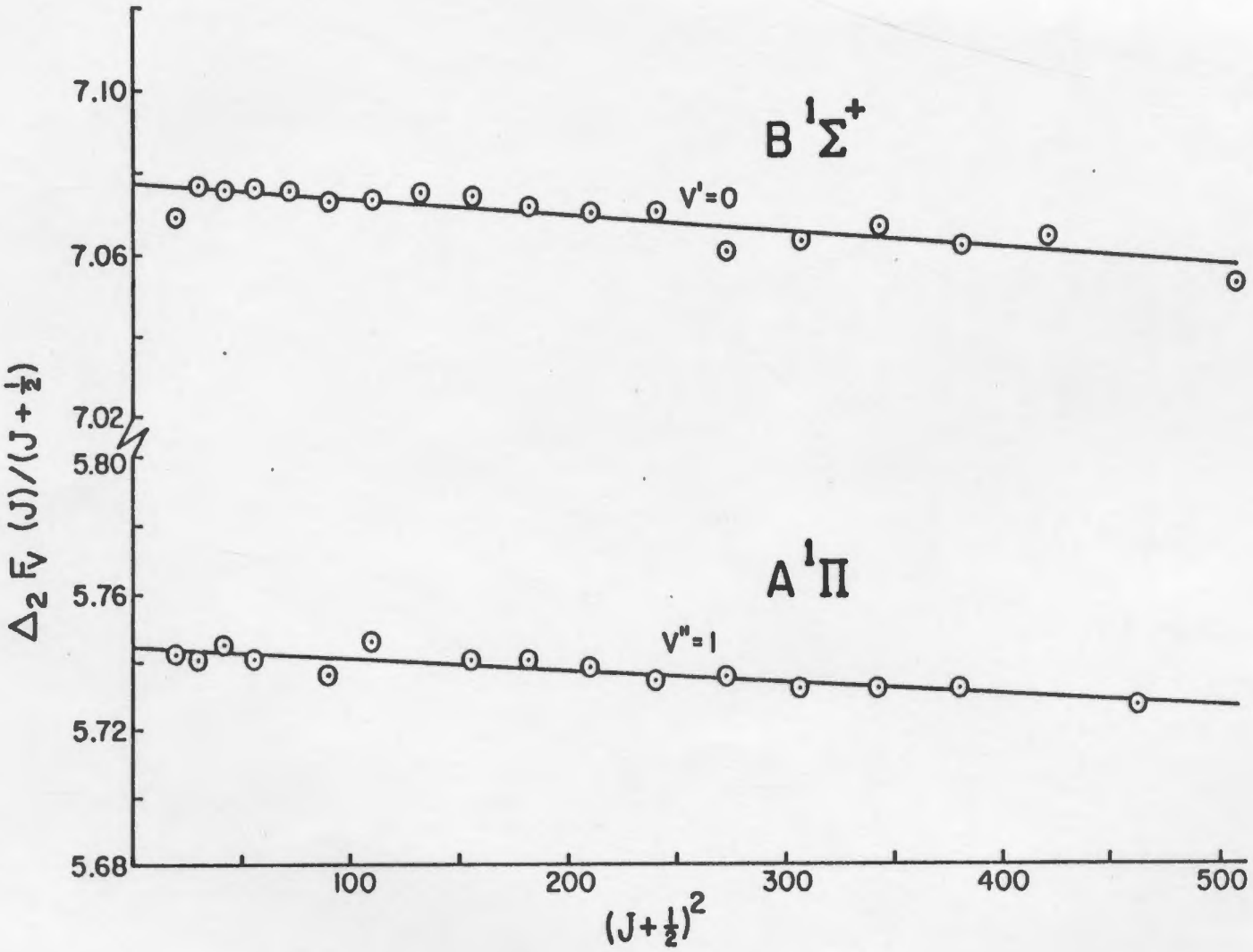

Fig. 14. Plots of $\Delta_2 F_v(J)$ / (J + 1/2) versus $(J + 1/2)^2$ for v' = 0 and v'' = 1 levels of the 0-1 band.

TABLE 2. Vacuum wavenumbers (in cm^{-1}) of the rotational lines of the 0-1 band

J	R(J)	Q(J)	P(J)
1	———	20742.01	20738.38
2	20753.87	20743.29	20736.23
3	20759.43	20745.30	20734.70
4	20765.66	20748.01	20733.85
5	20772.51	20751.30	20733.59
6	20780.08	20755.32	20734.09
7	20788.24	20759.99	20735.17
8	20797.13	20765.34	20737.03
9	20806.69	20771.30	20739.50
10	20816.91	20778.03	20742.64
11	20827.72	20785.33	20746.36
12	20839.25	20793.30	20750.83
13	20851.43	20801.96	20755.97
14	20864.27	20811.29	20761.76
15	20877.81	20821.25	20768.23
16	20891.89	20831.90	20775.40
17	20906.78	20843.18	20783.18
18	20922.32	20855.22	20791.59
19	20938.45	20868.01	20800.75
20	20955.37	20881.17	20810.56
21	20972.77	20895.19	20821.25
22	20990.92	20909.80	20832.24
23		20925.14	
24		20941.20	
25		20957.75	
26		20975.24	

TABLE 3. Vacuum wavenumbers (in cm^{-1}) of the rotational lines of the 0-2 band

J	R(J)	Q(J)	P(J)
1	19367.46	19360.52	19356.92
2	19372.43	19361.92	19354.81
3	19378.10	19364.09	19353.41
4	19384.47	19366.89	19352.70
5	19391.53	19370.42	19352.70
6	19399.35	19374.66	19353.41
7	19407.84	19379.67	19354.81
8	19417.04	19385.09	19356.92
9	19426.97	19391.53	19359.70
10	19437.51	19398.58	19363.24
11	19448.83	19406.35	19367.46
12	19460.81	19414.82	19372.43
13	19473.55	19424.01	19378.10
14	19486.93	19433.90	19384.47
15	19501.08	19444.46	19391.53
16	19515.84	19455.79	19399.35
17	19531.42	19467.74	19407.84
18	19547.76	19480.53	19417.04
19	19564.76	19494.01	19426.97
20		19508.16	19437.51
21		19522.93	
22		19538.63	
23		19555.06	
24		19572.26	

TABLE 4. Vacuum wavenumbers (in cm^{-1}) of the rotational lines of the 0-3 band

J	R(J)	Q(J)	P(J)
1	18016.72	18009.20	18006.04
2	18022.50	18011.93	18004.81
3	18028.42	18010.27	18003.64
4	18035.20	18014.47	18003.36
5	18042.96	18018.26	18004.03
6	18051.32	18023.57	18005.35
7	18054.56	18029.34	18001.48
8	18065.50	18035.69	18005.35
9	18076.43	18042.96	18009.20
10	18087.72	18052.11	18013.45
11	18099.65	18056.29	18018.26
12	18112.27	18065.94	18023.86
13	18125.44	18075.79	18029.96
14	18139.55	18086.43	18037.03
15	18154.31	18097.70	18044.75
16	18169.77	18109.69	18053.20
17	18186.03	18122.37	18062.38
18	18202.99	18135.86	18072.26
19	18220.71	18150.06	18082.96
20	18239.14	18165.01	18094.41
21		18180.71	18106.57
22		18197.11	
23		18214.30	
24		18232.33	

TABLE 5. Vacuum wavenumbers (in cm^{-1}) of the rotational lines of the 0-4 band

J	R(J)	Q(J)	P(J)
1	16697.27	16690.16	16686.63
2	16702.35	16691.76	16684.67
3	16708.24	16694.08	16683.47
4	16714.94	16697.27	16683.08
5	16722.38	16701.19	16683.47
6	16730.69	16705.92	16684.67
7	16739.73	16711.38	16686.63
8	16749.53	16717.70	16689.38
9	16760.14	16724.73	16692.95
10	16771.55	16732.61	16697.27
11	16783.67	16741.23	16702.35
12	16796.61	16750.66	16708.24
13	16810.36	16760.88	16714.94
14	16824.91	16771.88	16722.38
15	16840.16	16783.67	16730.69
16	16856.24	16796.24	16739.73
17	16873.20	16809.56	16749.53
18	16890.82	16823.77	16760.14
19	16909.30	16838.68	16771.55
20	16928.53	16854.45	16783.67
21	16948.58	16870.96	16796.61
22	16969.34	16888.23	16810.36
23		16906.40	16824.91
24		16924.96	16840.16
25		16944.85	16856.24
26		16965.31	

TABLE 6. Vacuum wavenumbers (in cm^{-1}) of the rotational lines of the 0-5 band

J	R(J)	Q(J)	P(J)
1	———	15403.07	15399.53
2	15415.32	15404.71	15397.62
3	15421.36	15407.20	15396.60
4	15428.20	15410.52	15396.36
5	15435.87	15414.66	15396.94
6	15444.38	15419.63	15398.37
7	15453.73	15425.43	15400.65
8	15463.86	15432.05	15403.73
9	15474.85	15439.49	15407.64
10	15486.68	15447.79	15412.40
11	15499.32	15456.92	15418.01
12	15512.83	15466.90	15424.45
13	15527.09	15477.77	15431.65
14	15542.31	15489.59	15439.79
15	15558.38	15503.38	15448.85
16	15575.40	15513.78	15458.89
17	15594.23	15528.34	15470.62
18	15608.51	15543.50	15477.77
19	15628.73	15559.47	15491.02
20	15649.38	15576.81	15504.66
21		15592.10	15518.81
22		15610.88	15533.46
23		15630.17	
24		15650.34	

TABLE 7. vacuum wavenumbers (in cm^{-1}) of the rotational lines of the 1-1 band

J	R(J)	Q(J)	P(J)
1	22736.02	22729.02	22725.62
2	22740.93	22730.31	22723.29
3	22746.24	22732.13	22721.68
4	22752.12	22734.65	22720.63
5	22758.67	22737.74	22720.53
6	22765.90	22741.44	22720.53
7	22773.77	22745.80	22721.38
8	22782.30	22750.77	22722.85
9	22791.33	22756.37	22725.00
10	22800.97	22762.62	22727.61
11	22811.32	22769.40	22731.00
12	22822.29	22776.89	22734.99
13	22833.87	22784.98	22739.63
14	22846.10	22793.66	22744.82
15	22858.66	22802.96	22750.77
16	22872.12	22812.91	22757.17
17	22886.18	22823.49	22764.16
18	22900.82	22834.67	22771.87
19	22916.17	22846.40	22780.19
20	22931.88	22858.87	22789.17
21	22948.43	22872.12	22798.64
22		22886.18	
23		22900.82	

TABLE 8. Vacuum wavenumbers (in cm^{-1}) of the rotational lines of the 1-0 band

J	R(J)	Q(J)	P(J)
1	———	———	———
2	———	———	———
3	———	———	———
4	———	24141.56	———
5	24163.97	24144.58	———
6	24171.73	24149.06	———
7	24180.28	24154.56	24127.35
8	24188.73	24153.50	24128.97
9	24197.77	24159.92	24131.61
10	24207.34	24166.48	24134.77
11	24212.74	24173.23	24132.42
12	24223.77	24180.28	24136.37
13	24235.81	24187.81	24141.56
14	24248.06	24195.75	24146.64
15	24260.01	24204.27	24152.12
16	24272.80	24213.30	24157.09
17	24285.88	24222.98	24163.97
18	———	24233.48	24170.33
19	24314.79	24244.25	24178.29
20	24328.96	24255.82	24185.31
21	24344.03	24267.72	24194.40

TABLE 9. Molecular constants of the $A\,^1\Pi$ and $B\,^1\Sigma^+$ states of $^{13}C\,^{18}O$

Molecular Constant	$A\,^1\Pi$	$B\,^1\Sigma^+$
ω_e (cm^{-1})	1444.49	2012.97
$\omega_e x_e$ (cm^{-1})	15.73	12.95
B_0 (cm^{-1})	1.4616(4)	1.7695(3)
B_1 (cm^{-1})	1.4356(3)	1.7476(6)
B_2 (cm^{-1})	1.4160(6)	
B_3 (cm^{-1})	1.3953(3)	
B_4 (cm^{-1})	1.3759(3)	
B_5 (cm^{-1})	1.3551(6)	
B_e (cm^{-1})	1.4660(5)	1.7805(4)
α_e (cm^{-1})	0.0201(1)	0.0219(6)
D_e (cm^{-1})		$5.0(8)\times10^{-6}$
D_0 (cm^{-1})	$4.2(8)\times10^{-6}$	$7.0(1.1)\times10^{-6}$
D_1 (cm^{-1})	$5.5(1.3)\times10^{-6}$	
D_2 (cm^{-1})	$6.5(2.5)\times10^{-6}$	
D_5 (cm^{-1})		
r_0 (Å)	1.2360	1.1233
r_1 (Å)	1.2471	1.1303
r_2 (Å)	1.2557	
r_3 (Å)	1.2650	
r_4 (Å)	1.2739	
r_5 (Å)	1.2836	
r_e (Å)	1.2350	1.1198
I_e ($gm.cm^2$)	1.909×10^{-39}	1.572×10^{-39}
T_e (cm^{-1})	65075.72[a]	86945.2[a]

$$\nu_e = T'_e - T''_e = 21869.43 \text{ cm}^{-1}$$

a Data taken from Tilford and Simmons (1972).

in Fig.15. The derived values of ν_0 and $(B'_v - B''_v)$ are listed in Table.10. The rotational constants B_0 and B_3 of the lower state could not be obtained from Eq.(3.23) because of the perturbations. They were calculated using the $(B_1 - B_0)$ and $(B_0 - B_3)$ differences obtained from the Q-branches of the 1-0 and 0-3 bands and the B_1 and B_0 values of the upper state respectively. Hence the centrifugal stretching constants D_0 and D_3 could not be calculated. As the R and P branches were completely overlapped in the 0-4 band, the D_4 value could not be computed accurately. The B_0 and B_3 values are also listed in Table.9. The perturbations were observed for certain J values in the 1-0, 0-3, and 0-5 bands. These perturbations will be discussed at length in Chapter 4. In the calculations of the rotational constants, the data in the perturbed regions were excluded.

The equilibrium rotational constants B_e and α_e of the $A\,^1\Pi$ state were obtained by linear least squares fit of B_v values against $(v + 1/2)$ (Ref. Eq.(3.5)). The values of B_e and α_e of $B\,^1\Sigma^+$ were calculated from B_0 and B_1. The equilibrium internuclear distances (r_e) and the moments of inertia (I_e) for both the electronic states were calculated using Eq.(3.6).The values of B_e, α_e, r_e, and I_e of both the states are also listed in Table.9.

3.4 Vibrational Constants from the Band Origins

The band origins of all the bands, except the 0-0 band, were directly obtained from the analyses of their Q-branches. The corresponding value of the 0-0 band was interpolated from those of 1-0, 1-1, and 0-1 bands. The values of the band origins are arranged in the Deslandres scheme in Table.11. Since the 1-0, 0-0, and 0-3 bands are shifted from their

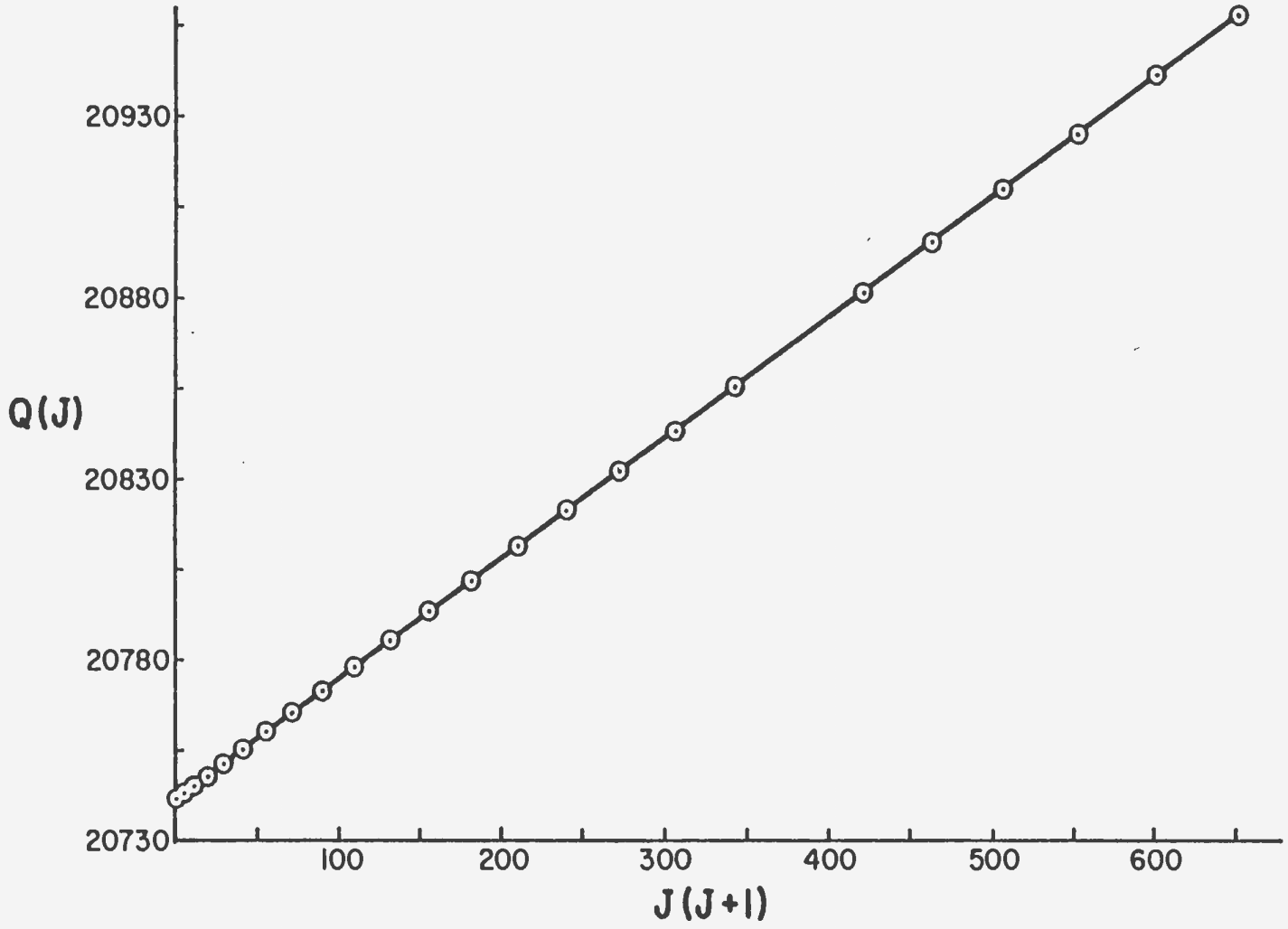

Fig. 15. A plot of Q(J) (in cm^{-1}) of the 0-1 band versus J(J+1).

TABLE 10. Band origins and $(B'_v - B''_v)$ values of the Ångström bands of $^{13}C\,^{18}O$

Band v'-v''	Band Origin (cm^{-1})	$B'_v - B''_v$ (cm^{-1})
1-0	24135.61(9)	0.2860(3)
1-1	22728.41(1)	0.3107(1)
0-1	20741.34(1)	0.3330(1)
0-2	19359.78(2)	0.3532(1)
0-3	18007.79(8)	0.3742(2)
0-4	16689.37(1)	0.3930(1)
0-5	15402.21(1)	0.4147(2)

TABLE 11. Deslandres scheme for the Ångström bands of $^{13}C\,^{18}O$

v' \ v''	0	1	2	3	4	5
		1381.56			1287.16	
0	22148.54[a,b]	20741.34	19359.78	18007.79[b]	16689.37	15402.21
		1987.07				
1	24135.61[b]	22728.41				

a Interpolated from neighboring values.

b Origins are shifted due to perturbations.

expected positions because of the perturbations, their origins could not be used in deriving the vibrational constants. The values of $\Delta G(3/2)$ and $\Delta G(9/2)$ obtained from the unperturbed origins of the 0-1, 0-2, 0-4, and 0-5 bands were used to calculate ω_e and $\omega_e x_e$ of the $A\,^1\Pi$ state from the relation

$$\Delta G(v + 1/2) = \omega_e - 2\omega_e x_e (v + 1/2) \qquad (3.25)$$

The quantities ω_e and $\omega_e x_e$ for the upper state ($B\,^1\Sigma^+$) were calculated from Eq.(3.9) by making use of the values of ω_e and $\omega_e x_e$ of the A state obtained above and the value of the system origin obtained by Tilford and Simmons (1972) for $^{12}C\,^{16}O$. Finally all the derived vibrational constants of the $^{13}C\,^{18}O$ are summarized in Table.9. As the data used to obtain these constants is limited, much accuracy can not be claimed. However, with these constants the band origins are reproduced to within 1.6 cm^{-1}.

The values of ω_e, $\omega_e x_e$, B_e, and α_e for states A and B of $^{13}C\,^{18}O$ were also calculated from the corresponding values of $^{12}C\,^{16}O$ as given by Tilford and Simmons (1972) using the formulae

$$\omega_e = \rho\,(\omega_e)^{12}C\,^{16}O$$

$$\omega_e x_e = \rho^2\,(\omega_e x_e)^{12}C\,^{16}O$$

$$B_e = \rho^2\,(B_e)^{12}C\,^{16}O$$

$$\alpha_e = \rho^3\,(\alpha_e)^{12}C\,^{16}O$$

$$\text{where } \rho = \left[\frac{\mu^{12}C\,^{16}O}{\mu^{13}C\,^{18}O}\right]^{1/2}$$

$$= 0.952986 \quad .$$

The observed and the calculated values are listed in Table.12 and the agreement between them is found to be very satisfactory.

TABLE 12. Comparison of the observed and calculated molecular constants of B and A states of $^{13}C^{18}O$ molecule

Molecular	$A\,^1\Pi$		$B\,^1\Sigma^+$	
Constant	Observed (cm^{-1})	Calculated (cm^{-1})	Observed (cm^{-1})	Calculated (cm^{-1})
ω_e	1444.49	1446.86	2012.97	2013.37
$\omega_e x_e$	15.73	17.62	12.95	13.80
B_e	1.4660	1.4635	1.7805	1.7811
α_e	0.0201	0.0201	0.0219	0.0226

CHAPTER 4

PERTURBATIONS IN THE $A\,^1\Pi$ STATE OF THE $^{13}C^{18}O$ MOLECULE.

Perturbations observed in the 0-3, 0-5, and 1-0 bands of the $B\,^1\Sigma^+ - A\,^1\Pi$ system of the $^{13}C^{18}O$ will be interpreted in this chapter. The theory of perturbations is briefly outlined in Sec.4.1. Perturbations caused in a $^1\Pi$ state by $^3\Sigma^+$ and $^3\Sigma^-$ states are discussed in Sec.4.2. The observed perturbations of the $A\,^1\Pi$ state of $^{13}C^{18}O$ are interpreted in Sec.4.3. Finally the information obtained for the perturbing states $a'\,^3\Sigma^+$ and $e\,^3\Sigma^-$ of $^{13}C^{18}O$ and the conclusions drawn are presented in the Sec.4.4.

4.1 Theory of Perturbations

In general, the wavenumbers ν (in cm^{-1}) of the rotational lines of a given branch of a band in an electronic transition can be represented by

$$\nu = a + bJ + cJ^2 + \ldots\ldots \qquad (4.1)$$

However, when perturbations occur, a rotational line or a series of successive lines deviate considerably from Eq.(4.1) and hence deviations from the smooth course of the branches are observed. For a certain types of perturbations in addition to the deviations, weakening in intensity may also appear. In general these deviations increase to a maximum with increasing J and suddenly change sign and then increase to zero and continue to follow the regular smooth course of the branch.

If E_1 and E_2 are two closely lying unperturbed energy levels of a molecule and E_a and E_b are the corresponding perturbed levels of E_1 and

E_2 respectively, then

$$E_{a,b} = \frac{E_1 + E_2}{2} \pm 1/2 \left[4(W_{12})^2 + \delta^2\right]^{1/2} \quad (4.2)$$

where $\delta = E_1 - E_2$ is the separation of the unperturbed levels and W_{12} is the matrix element of the perturbation function W, which is either an additional term in the potential energy or an operator due to the additional term in kinetic energy (Herzberg 1950, P. 13). The shifts in the levels, i.e., $(E_a - E_1)$ and $(E_b - E_2)$ are equal in magnitude and opposite in sign. Generally the levels E_1 and E_2 belong to two different electronic states of the molecule. The shifts in the energy levels are schematically shown in Fig.16.

Based on theoretical considerations Kronig (1928) derived the selection rules for the occurrence of perturbations between two energy levels.

(1) The rotational quantum number J must be the same for both the levels, i.e., $\Delta J = 0$.

(2) The resultant spin S of the two states may differ by 0 or ±1, i.e., $\Delta S = 0, \pm 1$. For example, a singlet state can be perturbed by either a singlet state or a triplet state.

(3) The components of the orbital angular momentum along the internuclear axis of the two states can differ only by 0 or ±1, i.e., $\Delta \Lambda = 0, \pm 1$.

According to Mulliken (1937), if $\Delta \Lambda = 0$, the perturbation is called homogeneous and if $\Delta \Lambda = \pm 1$, heterogeneous perturbation. The general behavior of the deviations of the rotational lines in the neighborhood of the point of maximum perturbation as a function of the rotational quantum

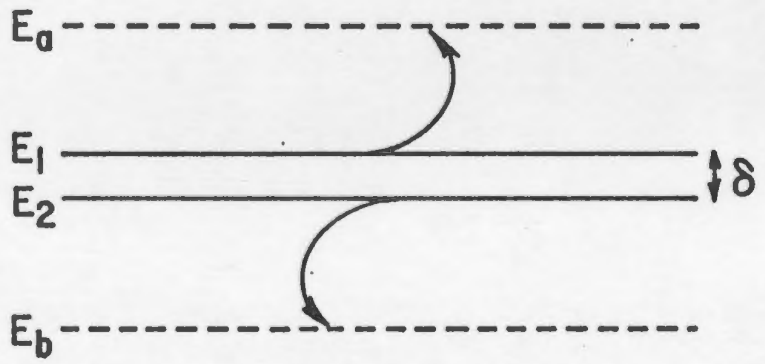

Fig. 16. A schematic diagram showing the shift of the energy levels E_1 and E_2. Generally, E_1 and E_2 belong to two different electronic states.

number is shown for homogeneous and heterogeneous perturbations in Fig.17. It is seen from this figure that in homogeneous perturbations, the deviations do not become zero when J=0, in contrast to the case of heterogeneous perturbations, so that the deviation appears as if the whole vibrational level were shifted. Because of this, the homogeneous perturbation is sometimes called vibrational perturbation and the other one is called rotational perturbation (Dieke 1941).

(4) Both the levels should have the same parity, i.e., either the positive or negative, i.e., $+ \not\leftrightarrow -$ and in case of identical nuclei, both the levels must have the same symmetry, i.e., either symmetric or antisymmetric, i.e., $s \not\leftrightarrow a$.

For example, if two states having the $\Lambda-$ type doubling perturb each other, the rotational lines in all the branches are affected similarly and hence the maximum perturbation occurs at the same J in all the three branches. In contrast to this, if an electronic state having $\Lambda-$ type doubling is perturbed by a state not having this type of splitting in its rotational levels, for example a $\Pi - \Sigma$ perturbation, its effect is not similar in all the branches. The perturbations caused by a Σ^+ state are different from those caused by a Σ^- state because of the difference in the parity of the rotational levels. If a $^1\Sigma^+ - {}^1\Pi$ transition is considered, (Fig.8) as the P and R lines end on one Λ - doublet component and the Q lines end on the other, the perturbations caused in this $^1\Pi$ state by a Σ state are similar in the P and R branches and different in the Q branch.

Sometimes, a heterogeneous perturbation in the low-lying rotational levels, produces a shift in the band origin and appears as if it were a vibrational perturbation. Basing on the points and magnitudes of perturbation in

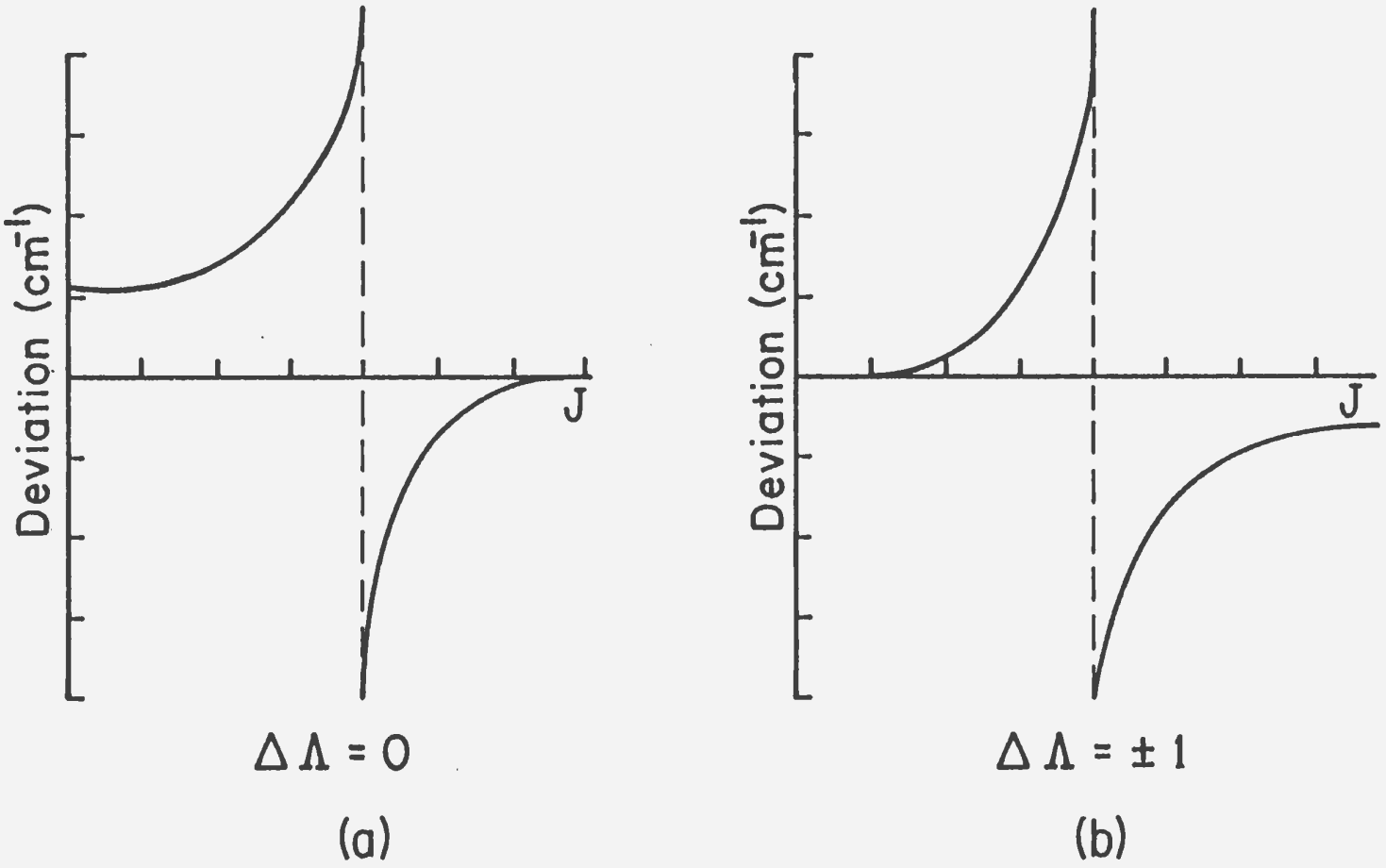

Fig. 17. Behavior of the deviation in rotational lines due to perturbations as a function of the rotational quantum number J in case of (a) homogeneous perturbations $\Delta\Lambda = 0$ and (b) heterogeneous perturbations $\Delta\Lambda = \pm 1$.

all the branches, it is to be decided whether it is a vibrational perturbation or not. For example, Marais (1946) observed a rotational perturbation which caused a shift in the origins of the 5-20 and 5-21 bands due to the perturbations in v=5 level of $C\,^1\Sigma_u^+$ state of the P_2 molecule.

4.2 Perturbations in a $^1\Pi$ State by $^3\Sigma^+$ and $^3\Sigma^-$ States.

A Σ state does not have Λ- type doubling. Hence depending on the parity of its rotational levels, it perturbs only one of the Λ- doublet components of the Π state. Thus if a Σ^+ state perturbs one component, a Σ^- state perturbs the other component. The rotational levels and their parities of $^3\Sigma^+$ and $^3\Sigma^-$ states are schematically shown in Fig.18 and those of a $^1\Pi$ are given in Fig.8. In a $^3\Sigma$ state, each level, except the one with N=0,has three components with J values N-1, N, and N+1 where N is the total angular momentum apart from spin. For a given N, all the three levels with different J values have same parity, either positive or negative, and also they have about the same energy. But the three levels with the same J and different N are alternatively positive and negative. In general, if a singlet state is perturbed by a triplet state, maximum perturbation is expected at three different places. But as explained earlier, if a $^1\Pi$ state is perturbed by a Σ state, the perturbations in the P and R branches are similar and they are different from those in the Q branch. Hence if a $^1\Pi$ state is perturbed by a $^3\Sigma$ state the three perturbations in the P (and R) and Q branches will be at different rotational levels. Basing on the parity considerations it is established that any of the following two types of perturbations can occur in the increasing order of J.

(i) Perturbations in Q branch, P and R branches, and Q branch

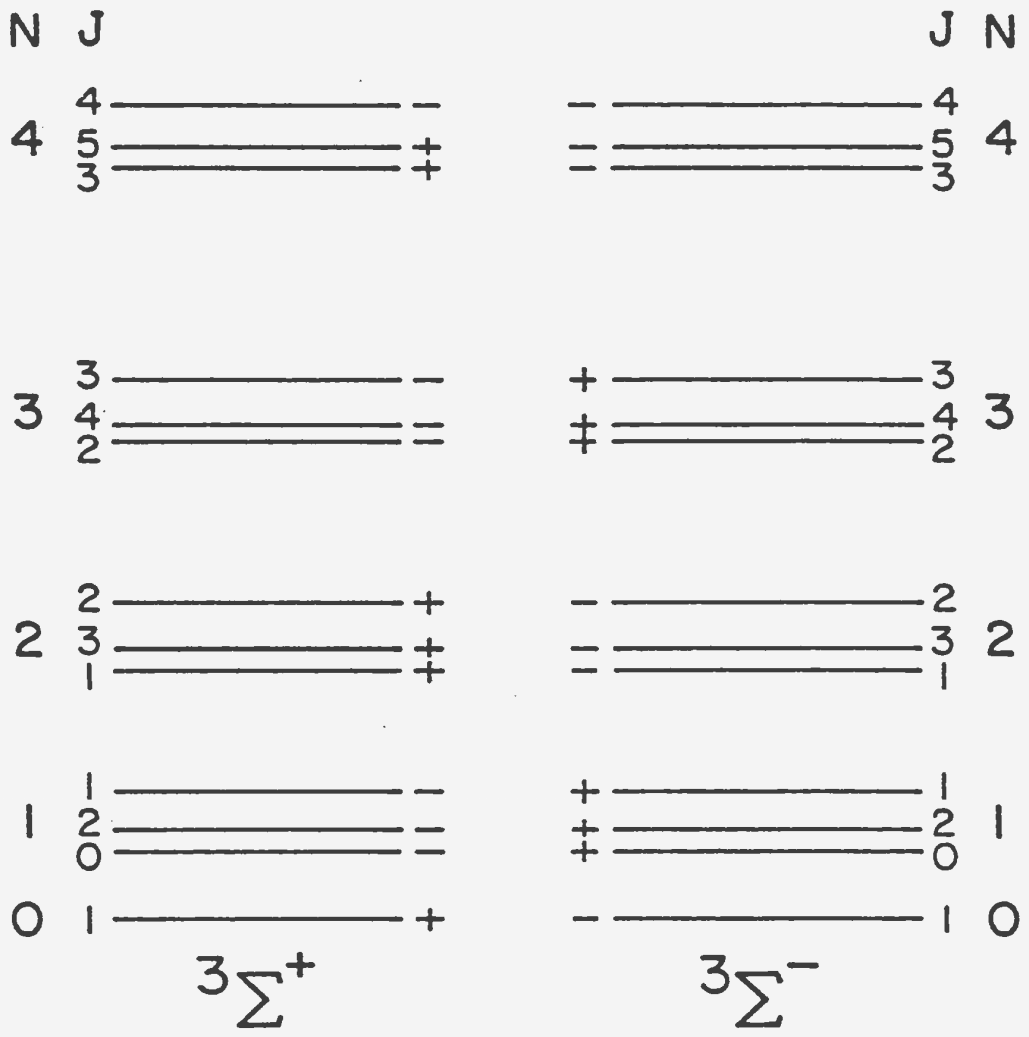

Fig. 18. Rotational levels (shown schematically) and their parities in $^3\Sigma^+$ and $^3\Sigma^-$ states.

(ii) Perturbations in P and R branches, Q branch, and P and R branches

If $^3\Sigma^+$ state causes one of these two types of perturbations the $^3\Sigma^-$ state causes the remaining type of perturbation.

4.3 Interpretation of the Observed Perturbations

Some irregularities are observed in the rotational structures of the 0-3, 0-5, and 1-0 bands. As no such irregularities are observed in the rotational structures of the 0-1, 0-2, 0-4, and 1-1 bands, it indicates that there are no perturbations in the v=0 and 1 levels of the $B\,^1\Sigma^+$ state. Hence it is clear that the vibrational levels v=0,3, and 5 of $A\,^1\Pi$ state are perturbed. The facts that no rotational analysis was possible for the 0-0 band and 1-0 band was analyzed partially indicate that the v=0 level of $A\,^1\Pi$ is strongly perturbed.

Using the values of B_0 and B_1 of the $B\,^1\Sigma^+$, B_0, B_3, and B_5 of the $A\,^1\Pi$ state (Table 9) and the origins of the 0-3, 0-5, and 1-0 bands (Table 10), the rotational lines of the three branches of these bands were calculated. The deviations of the observed wavenumbers of these rotational lines from the calculated ones are then plotted against J as shown in Figs.19, 20, and 21. As explained in Section 4.2, the deviations in the P and R branches are found to be similar but they are different from those in the Q branch.

In the 0-3 band, the perturbations are observed in the Q, P and R, and Q branches at J=2, 6, and 10 respectively. As the P and Q branches are perturbed at different J values, this can not be a $\Pi - \Pi$ or $\Pi - \Delta$ perturbation. Finally, on the considerations of parity and proximity of the

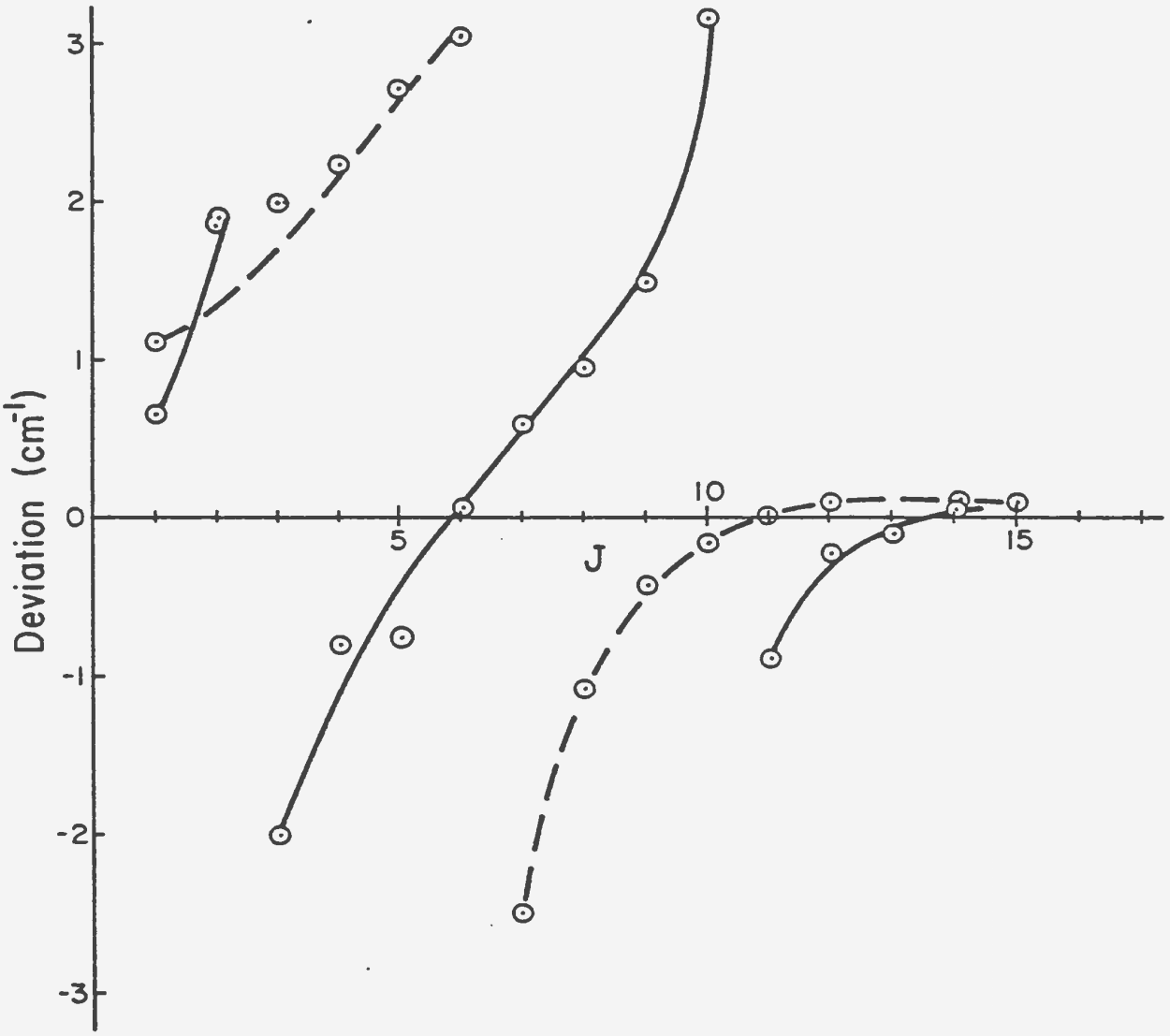

Fig. 19. Plots of deviations ($\nu_{obs} - \nu_{calc}$) of the rotational lines of the 0-3 band versus the rotational quantum number J. The solid curves represent the deviations in the Q branch and the dashed curves represent those in the P and R branches.

Fig. 20. Plots of deviations ($\nu_{obs} - \nu_{calc}$) of the rotational lines of the 0-5 band versus the rotational quantum number J. The solid curves represent the deviations in the Q branch and the dashed curves represent those in the P and R branches.

Fig. 20.

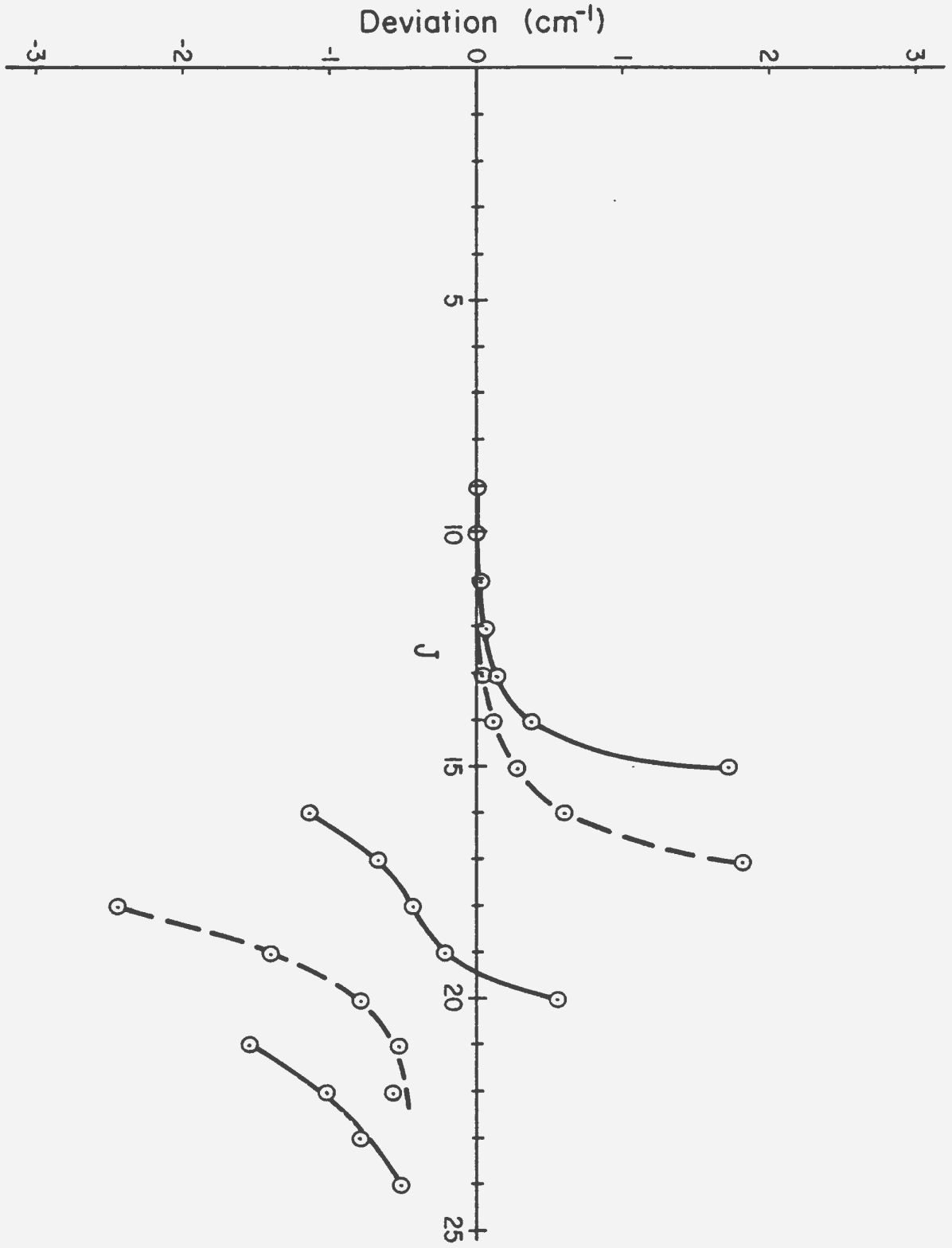
Deviation (cm⁻¹)
-3
-2
-1
0
1
2
3
J
5
10
15
20
25

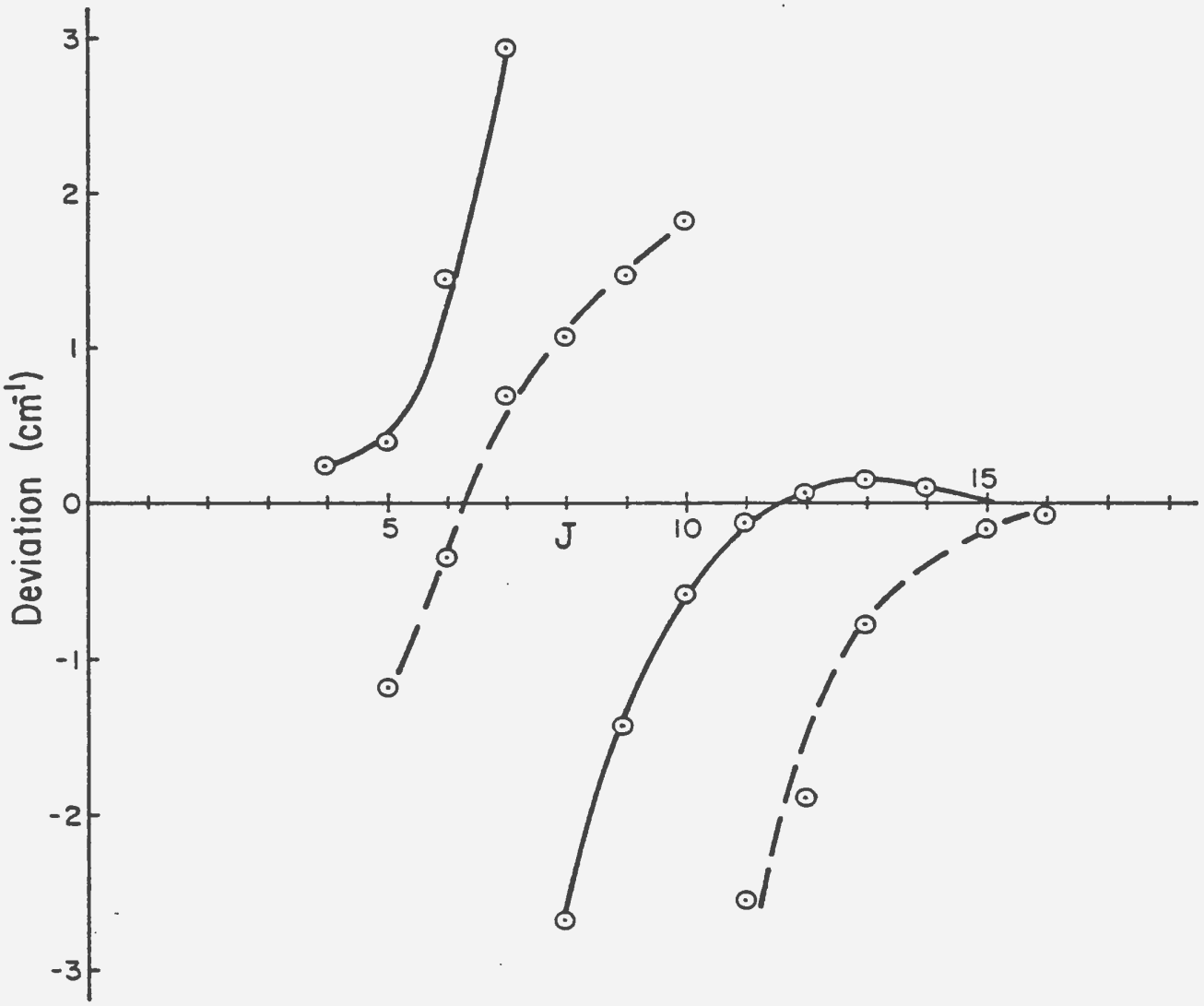

Fig. 21. Plots of deviations ($\nu_{obs} - \nu_{calc}$) of the rotational lines of the 1-0 band versus the rotational quantum number J. The solid curves represent the deviations in the Q branch and the dashed curves represent those in the P and R branches.

electronic states it is concluded that v=3 level of $A\,^1\Pi$ state is perturbed by $a'\,^3\Sigma^+$ state. But, though the difference, $\Delta\Lambda$, between the perturbed and the perturbing states is +1, the perturbation curves are similar to those of the $\Delta\Lambda = 0$ perturbation (see Fig.17). This is due to a shift in the band origin. If the origin is shifted by approximately +1.0 cm^{-1}, the calculated wavenumbers increase by +1.0 cm^{-1} and hence the differences between the observed and calculated wavenumbers decrease by the same amount uniformly in all the branches. Then these curves look similar to the perturbation curves of $\Delta\Lambda = \pm 1$ (see Fig.17). Hence it is clear that the origin of the 0-3 band is shifted due to the perturbations in the initial rotational levels.

From the perturbation curves drawn for the 0-5 band (see Fig.20), it is seen that the maximum perturbations occur at J=15, 18, and 21 in Q, P and R, and Q branches respectively. Hence as in the case of vibrational level v=3, the v=5 level of $A\,^1\Pi$ state is also found to be perturbed by the $a'\,^3\Sigma^+$ state. In this case, the perturbation curves are similar to those shown in Fig.17 for the case of $\Delta\Lambda = \pm 1$. As the initial rotational levels are not perturbed in the v=5 level, no significant shift in the origin of the 0-5 band is observed.

In the 1-0 band, as the spectral lines arising from the initial rotational levels are not identified, only two points of the maximum perturbations are observed at J=7 and 10 in the Q and P branches respectively. As there are no irregularities in the rotational lines belonging to the Q branch beyond J=11, the missing perturbation should be in the P and R branches around J=4. Hence in this band, perturbations in the P and R, Q, and P and R in the increasing order of J are expected. This type of perturbation

is opposite to the type observed in the 0-3 and 0-5 bands. Hence according to the theoretical considerations mentioned in Sec.4.2, the perturbing state in the v=0 level of $A\,^1\Pi$ is $e\,^3\Sigma^-$. In this band as the initial rotational levels are perturbed, a shift in the band origin is expected. As the spectral lines near the band head could not be assigned J numbering a quantitative estimate of the shift in the band origin could not be made.

4.4 Information Regarding the Perturbing States and Conclusions

To obtain the information about the perturbing states, the rotational term values F(J) of the perturbed vibrational levels v=0, 3, and 5 of the $A\,^1\Pi$ state are plotted against J. As an example, the plot drawn for the v=5 level is shown in Fig.22. In this figure the points of maximum perturbation shown on the solid curve are indicated at J=15, 18, and 21. At these points, according to Kronig's selection rule (1), the perturbing state will also have the same J values. For a $^3\Sigma$ state, there are three levels with same J having N values J-1, J, and J+1 (see Fig.18). Thus for J=15, there are three levels with N=14, 15, and 16. Among these, N=14 has the least energy. Among the points of maximum perturbation (J=15, 18, and 21) J=15 has the least energy. Hence, the perturbing J=15 level of $^3\Sigma$ has N=14. For N=14, all the three levels J=13, 14, and 15 have approximately the same energy. Similarly the rotational levels J=17, 18, and 19 corresponding to N=18 on one hand and J=21, 22, and 23 corresponding to N=22 on the other, have same energies respectively. The dashed curves in Fig.22 represent the energy curves for the components N = J-1, J, and J+1 of the $^3\Sigma$ state. From the energy curve of N=J in Fig.22, the rotational term values F(J) for different J and hence the corresponding B_v value of the perturbing state are obtained. The accuracy of the B_v value thus obtained

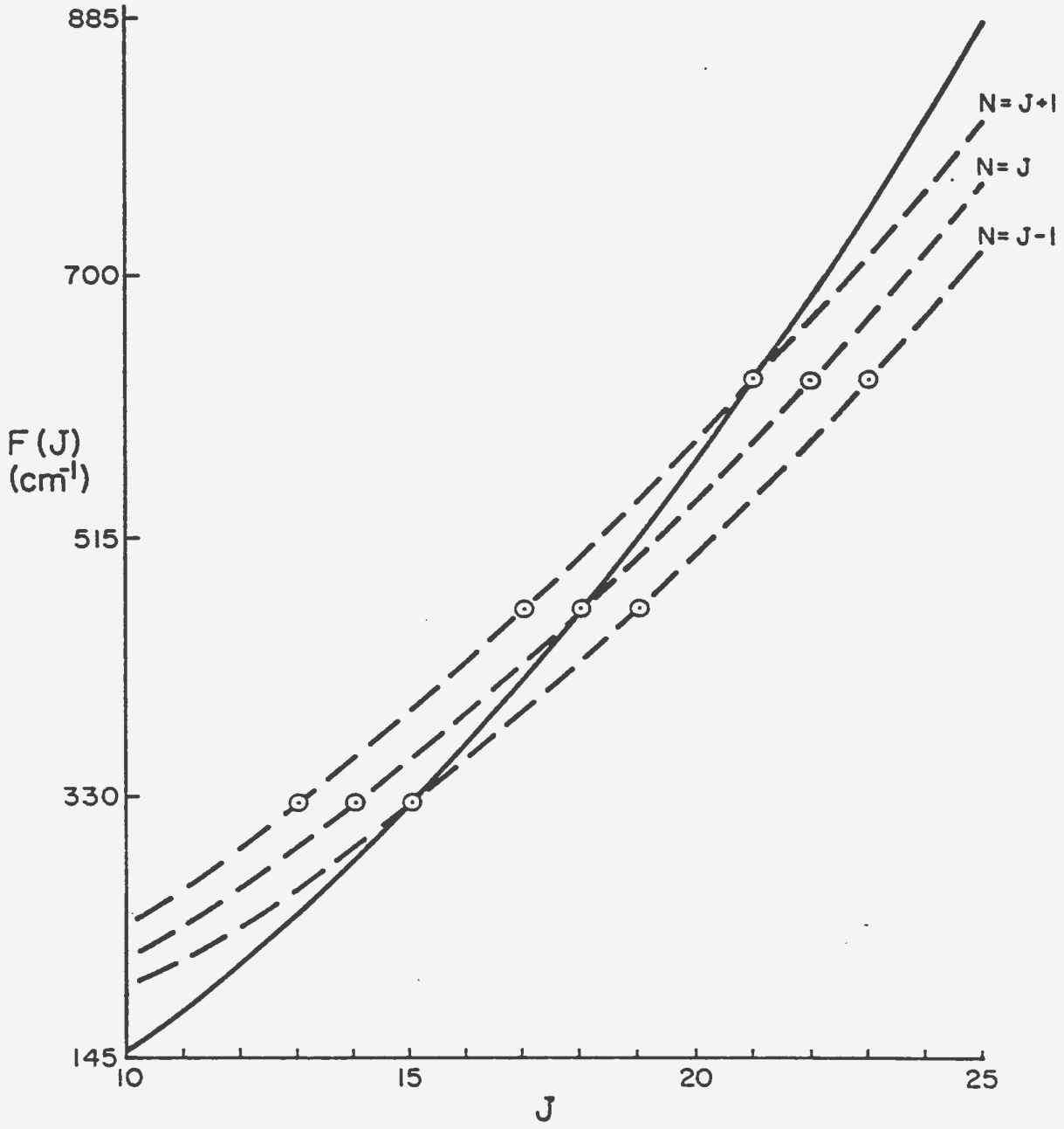

Fig. 22. Crossing of the v=5 level of the $A\,^1\Pi$ state by the $a'\,^3\Sigma^+$ state causing perturbations at J=15, 18, and 21.

for the perturbing state is somewhat less than that of the corresponding B_v value of the $A\,^1\Pi$ state.The values of B_v for the vibrational levels perturbing the v=0, 3,and 5 levels of $A\,^1\Pi$ are 1.074(7), 1.009(9), and 0.996(3) cm^{-1} respectively. These values are smaller than those of the $A\,^1\Pi$ state and hence only those vibrational levels which are slightly above the vibrational levels of the $A\,^1\Pi$ state can perturb the latter. From B_v values of the perturbing states and the energy values (T_e + G(v) + F_v(J)) of the perturbed levels at the points of maximum perturbation, the positions of the perturbing vibrational levels (T_e + G(v)) are calculated. These T_e + G(v) values of the perturbing levels belonging to the $a'\,^3\Sigma^+$ and $e\,^3\Sigma^-$ states of the $^{13}C\,^{18}O$ molecule are also calculated from the constants of $^{12}C\,^{16}O$ (Tilford and Simmons 1972) using the usual isotope relations. All these values are listed in Table 13 and the agreement between them is very satisfactory. It is found that the levels v=3 and 5 of $A\,^1\Pi$ are perturbed by the levels v=13 and 16 of $a'\,^3\Sigma^+$ respectively and the level v=0 of $A\,^1\Pi$ is perturbed by the level v=1 of $e\,^3\Sigma^-$. The vibrational levels of the $a'\,^3\Sigma^+$, $A\,^1\Pi$, and $e\,^3\Sigma^-$ states indicating the perturbed regions are shown in Fig.23.

From Fig.23 it is seen that the levels v=1, 2, and 4 of $A\,^1\Pi$ are not very close to the levels v=11, 12, and 15 of $a'\,^3\Sigma^+$ and v=3, 4, and 7 of $e\,^3\Sigma^-$ respectively. But these vibrational levels of a' and e states may cause perturbations in the v=1, 2, and 4 levels of state A at higher rotational levels. As the hollow cathode discharge tube used in the present study was operated at low currents, in general, the rotational levels with J > 25 are not excited. Hence the perturbations are not observed in the v=1, 2, and 4 levels of $A\,^1\Pi$ state for $J \leqslant 25$. Though the v=8 level of $e\,^3\Sigma^-$ is closer to the v=5 of $A\,^1\Pi$ than the v=16 of $a'\,^3\Sigma^+$ only the latter is causing perturbations in the v=5 level. The reason for this is that though the

TABLE 13. T_e + G(v) values of the perturbing levels of $a'^3\Sigma^+$ and $e^3\Sigma^-$ states of $^{13}C^{18}O$

Perturbed Level of $A^1\Pi$	Perturbing Level	T_e + G(v) Values	
		Observed (cm^{-1})	Calculated (cm^{-1})
v = 0	v = 1 of $e^3\Sigma^-$	65816.58	65806.48
v = 3	v = 13 of $a'^3\Sigma^+$	69956.05	69958.36
v = 5	v = 16 of $a'^3\Sigma^+$	72669.85	72667.46

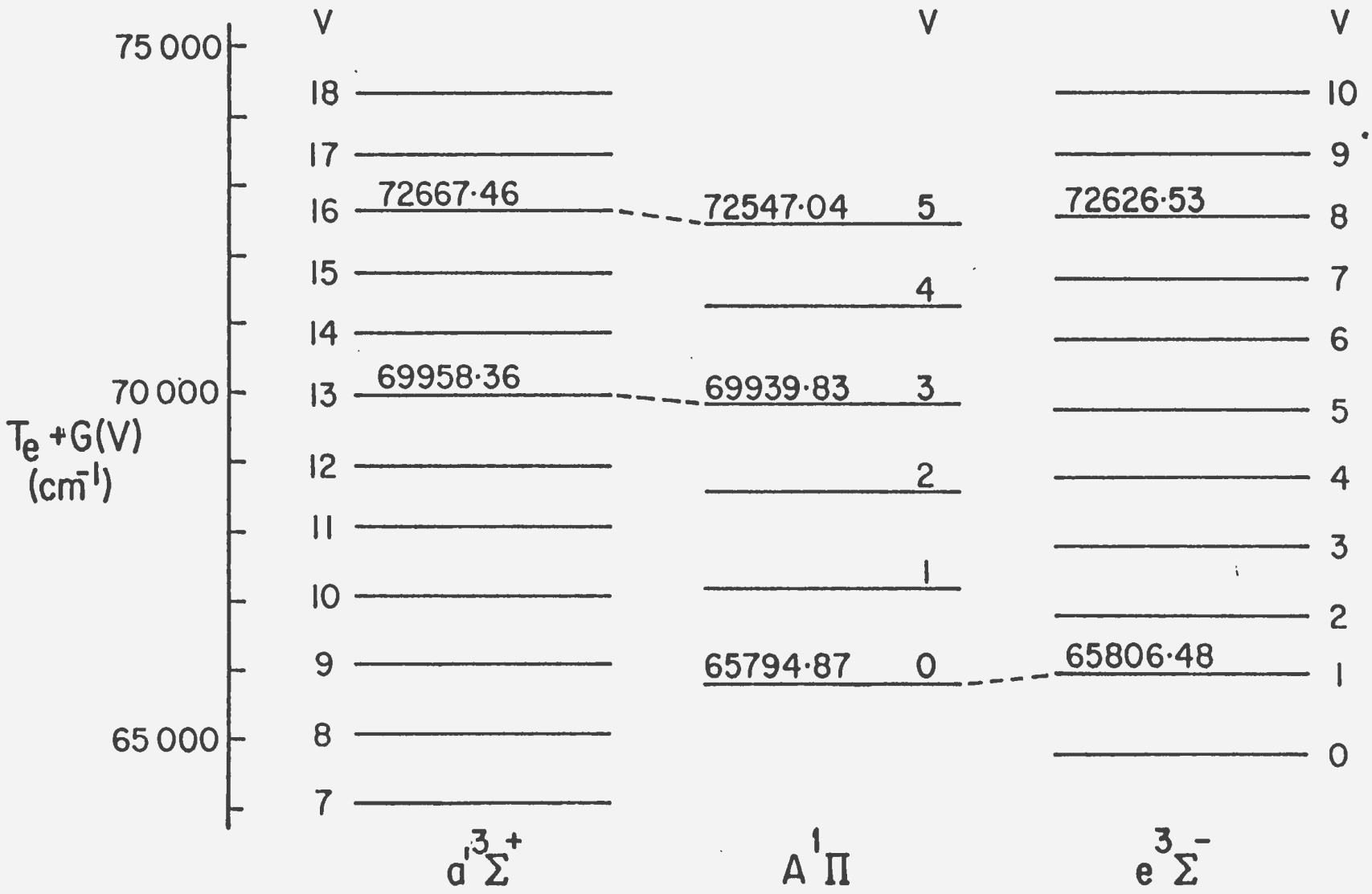

Fig. 23. Relative positions of the vibrational levels of the $a'^3\Sigma^+$, $A^1\Pi$, and $e^3\Sigma^-$ states of $^{13}C^{18}O$.

vibrational levels are closer, the potential energy curve of $e^3\Sigma^-$ state might not be crossing the curve of $A^1\Pi$ in the proximity of the v=5 level (see Herzberg 1950, P.286). In the case of v=0 level of $A^1\Pi$ state, as the perturbing level v=1 of $e^3\Sigma^-$ is very close (the difference between them is only 11.61 cm^{-1}) the initial rotational levels are strongly interacting and this could be the reason for the complicated structure of the rotational lines of the 1-0 band involving the first few rotational levels.

Coster and Brons (1934) studied the perturbations in the Ångström band system of the $^{12}C^{16}O$ molecule in detail and Rytel (1970 a, b) and Kepa and Rytel (1970) indicated the places of perturbations in the Ångström band systems of the $^{12}C^{16}O$, $^{13}C^{16}O$, and $^{12}C^{18}O$ molecules. According to these authors all the vibrational levels v = 0 to 5 of $A^1\Pi$ are perturbed in all the three molecular species mentioned here. But only the levels v=0, 3, and 5 of the $A^1\Pi$ state of $^{13}C^{18}O$ molecule are found to be perturbed in the present method of excitation.

REFERENCES

Asundi,R.K. Proc. Indian Acad. Sci., Sect.A. **3** , 554 (1936).

Bhogal,A.S. B.Sc thesis, Memorial University of Newfoundland (1982).

Birge,R.T. Physic. Rev. **28** , 1157 (1926).

Coster,D. and Brons,F. Physica **1** , 634 (1934).

Dieke,G.H. Physic. Rev. **60** , 523 (1941).

Douglas,A.E. and Møller,C.K. Can. J. Phys. **33** , 125 (1955).

Jasse,O. Compt. Rend. **182** , 692 (1926a).

Jasse,O. Rev. Opt. **5** , 450 (1926b).

Johnson,R.C. and Asundi,R.K. Proc. Roy. Soc. (London), Ser.A. **123** , 560 (1929).

Herzberg,G. Molecular Spectra and Molecular Structure, Vol I Second Edition. D. Van Nostrand Company, Inc., New York, (1950).

Herzberg,G., Lew,H., Sloan,J.J., and Watson,J.K.G. Can. J. Phys. **59** , 428 (1981).

Huber,K.P. and Herzberg,G. Molecular Spectra and Molecular Structure, Vol IV. Van Nostrand Reinhold Company, New York, (1979).

Hulthén,E. Ann. Physik. **71** , 41 (1943).

Hund,F. Z. Physik. **63** , 719 (1930).

Kepa,R. and Rytel,M. Acta Physica Polonica **A37** , 585 (1970).

Kepa,R. Rytel,M., Janjić,J.D., and Pešić,D.S. Acta Physica Polonica **A41** , 377 (1972).

Kronig, R de L. Z. Physik. **50** , 347 (1928).

Krupenie,P.H. The Band Spectrum of Carbon Monoxide (NSRDS - NBS 5) (1966).

Lefebvre - Brion,H., Moser,C.M., and Nesbet,R.K. J. Mol. Spectry. **13** , 418 (1964).

Marais,E.J. Physic. Rev. **70** , 499 (1946).

McCulloh,K.E. and Glockler,G. Phys. Rev. **89** , 145 (1953).

Mulliken,R.S. Rev. Mod. Phys. **4** , 1 (1932).

Mulliken,R.S. J. Phys. Chem. **41** , 5 (1937).

Rosenthal,J.E. and Jenkins,F.A. Proc. Nat. Ac. Am. **15** , 896 (1929).

Rytel,M. Acta Physica Polonica **A37** , 559 (1970a).

Rytel,M. Acta Physica Polonica **A38** , 299 (1970b).

Schmid,R. and Gerö,L. Z. Physik. **93** , 656 (1935).

Tilford,S.G. and Simmons,J.D. J. Phys. Chem. Ref. Data **1** , 147 (1972).

GENERAL REFERENCES

Crosswhite,H.M. Johns Hopkins Spectroscopic Report Number 13 (1958).

Crosswhite,H.M. Journal of Research of the National Bureau of Standards - A. Physics and Chemistry **79A** , 17 (1975).

Gatterer,A. and Junkes,J. Arc Spectrum of Iron. Specola Vaticana, Citta Del Vaticano, (1956).

Herzberg,G. Molecular Spectra and Molecular Structure, Vol I Second Edition. D. Van Nostrand Company, Inc., New York, (1950).

Huber,K.P. and Herzberg,G. Molecular Spectra and Molecular Structure, Vol IV. Van Nostrand Reinhold Company, New York, (1979).

Kovács,I. Rotational Structure in the Spectra of Diatomic Molecules. American Elsevier Publishing Company, Inc., New York, (1969).

Mulliken, R.S., "Interpretation of Band Spectra",

Part I, II(a), and II(b), Rev. Mod. Phys. **2** , (1930).

Part II(c) Rev. Mod. Phys. **3** , (1931).

Part III Rev. Mod. Phys. **4** , (1932).

Pearse,R.W.B. and Gaydon,A.G. The Identification of Moleculer Spectra, Third Edition. Chapman & Hall Ltd., London, (1963).